"Alma Mater Studiorum" Bologna University

Physics Department

PhD in Geophysics

XXIV Cycle

04/04

Reconstruction of Etna recent flank eruptions for assessing diversion barrier project

Silvia Scifoni

PhD Coordinator:
Prof. Michele Dragoni

Tutor:
Prof.ssa Maria Marsella
Co-tutor:
Dr. Mauro Coltelli

2012

Contents

List of Figures

List of Tables

Abstract

Volcanic risk is the combination of hazard associated to dangerous and/or destructive volcanic phenomena, and exposure of people and/or properties living in the involved areas. The assessment of volcanic hazard, i.e. the probability that given areas will be affected by potentially destructive volcanic processes, represents one of the most important goals of current volcanology with an immediate and practical impact on society. It is based on reconstruction of the eruptive record, monitoring of the present state of the volcano, modelling and simulating of the volcanic process and quantification of the system uncertainty.
The thesis contributed to the volcanic hazard assessment through the reconstruction of some historical flank eruptions of Etna in order to obtain quantitative data (volumes, effusion rates, etc.) for characterizing the recent effusive activity, quantifying the impact on the territory and defining mitigation actions for reducing the volcanic risk as for example containment barriers. The reconstruction was based on a quantitative approach using data extracted from aerial photographs and topographic maps. The approach consists in defining the final lava flow field using orthophotos or historical maps, estimating the final volumes by subtraction of the pre- and post- eruption Digital Elevation Models (DEM), reconstructing the temporal evolution of the lava flow field and estimating the Time Average Discharge Rate (TADR) by dividing the volume emplaced over a given time interval for the corresponding duration. From the TADR reconstruction it was possible to evaluate the peak value that represents a fundamental parameter for the Civil Protection because it provides an estimation of response time for the intervention. The analysis concerned the 2001, 1981 and 1928 Etna eruptions. The choice of these events is linked to their impact on inhabited areas. In fact in 1928 the town of Mascali was completely destroyed and in 1981 Randazzo was threatened by lava flows. As to the 2001 eruption, it was chosen because during this event earthen

barriers were built, therefore it represents a good test to evaluate this type of actions. The results of the analysis showed an extraordinarily high effusion rate for the 1981 and 1928 eruptions (over 600 m^3/s), unusual for Etna eruptions. For the 1981 Etna eruption a semi-quantitative model of the eruptive mechanisms was proposed to explain the high average effusion rate. The obtained TADRs were used as input data for simulations of the propagation of the lava flows. The aim of the simulations performed for the 1981 eruption was evaluating different scenarios of volcanic hazard, while those performed for the 2001 eruption were intended to analyse different mitigation actions against lava flow invasion. Furthermore, an engineering approach for the positioning and building of the containment barriers was adopted in this work. In particular, it was experienced how numerical simulations could be adopted for evaluating the effectiveness of barrier construction and for supporting their optimal design. The dynamical and thermal models that describe the lava flow front-barrier interaction were fully investigated in order to dimension the structure. A finite element model was implemented that allowed an estimation of the pressure of the lava flow on the barrier. Based on these results, the gabions were proposed as an improvement for the construction of barriers with respect to the earthen barriers. The gabion barriers allow to create easily modular structures reducing the handled volumes and the intervention time. For evaluating operational constrain an experimental test was carried out to test the filling of the gabions with volcanic rock and evaluating their deformation during transport and placement.

Chapter 1

Introduction

Mount Etna is located in the eastern part of Sicily Island (Italy) and it is the largest active volcano in Europe. Eruptions of Etna are not always the same. Most occur at the summit, where there are four distinct craters (the Northeast Crater, the Voragine, the Bocca Nuova, and the South-east Crater). They are characterized by Strombolian eruptions and periodic lava fountaining episodes, often associated with lava flows. These eruptions are rarely threatening for the inhabited areas around the volcano. In this case the main hazard is represented by earthquake and ash-fall. Other eruptions occur on the flanks and can reach altitude of a few hundred meters close to or even well within the populated areas. The most destructive events were the 1669 and the 1928 eruptions. In 1669 the lava field, whose lowest vent opened at 900 m a.s.l. on the southern flank, caused extensive damage to the city of Catania and reached the sea. In 1928 the lava emitted from vents at 1200 m a.s.l. reached and covered the town of Mascali. More recently in 1971, the lava buried the Etna Observatory (built in the late 19th century), destroyed the first generation of the Etna cable-car and seriously threatened several small villages on Etna's east flank. In March 1981, the town of Randazzo on the northwestern flank of Etna just escaped from destruction by an unusually fast moving lava flow, an eruption remarkably similar to the one in 1928 that destroyed Mascali. In the 1983 eruption a fissure on the south flank of the volcano produced a lava flow that destroyed several restaurants, chalets, and small buildings and threatened three towns downhill. The 1991-1993 eruption saw the town of Zafferana threatened by a lava flow but successful diversion efforts

saved the town with the loss of only one building a few hundred metres from the town's margin. Following six years (1995-2001) of activity at the four summit craters of Etna, the volcano produced its first flank eruption after the 1991-1993 event in July-August 2001. Part of the "Etna Sud" tourist area, including the arrival station of the Etna cable car, were damaged by this eruption. During this event 13 earth barriers were build to protect the tourist area. In 2002-2003, a much larger eruption occurred. Seismic activity in this eruption caused structural damage to houses on the volcanoes flanks. The eruption completely destroyed also the tourist station "Piano Provenzana" on the northeastern flank of the volcano, and part of the tourist station "Etna Sud" around the "Rifugio Sapienza" on the south flank. An eruption on the morning of 13 May 2008, immediately to the east of Etna's summit craters was accompanied by a swarm of more than 200 earthquakes and significant ground deformation in the summit area. The eruption continued at a slowly diminishing rate for 417 days, until 6 July 2009, making this the longest flank eruption of Etna since the 1991-1993 eruption that lasted 473 days. It should be noted that these eruptions, as well as all the eruptions inside the "Valle del Bove", rarely threaten the inhabited areas if they remains confined within the depression. From this brief overview of Etna flank eruptions it is clear that studying this type of events is a fundamental tool for assessing the associated volcanic risk.

Chapter 2

Analysis of Etna historical flank eruptions

This chapter describes the method applied for the reconstruction and the TADR trend estimation of 2001, 1981 and 1928 Etna eruptions. A brief chronology and the description of quantitative data are reported for each event. The 1981 and 1928 are totally reconstructed. As concern the 2001 eruption the lava flows from the fissure at the 2770 m a.s.l. and the vent at the 2550 m a.s.l. are reconstructed because against them 13 earth barrier were built, representing a good case (for our scope) to evaluate the barrier efficiency.

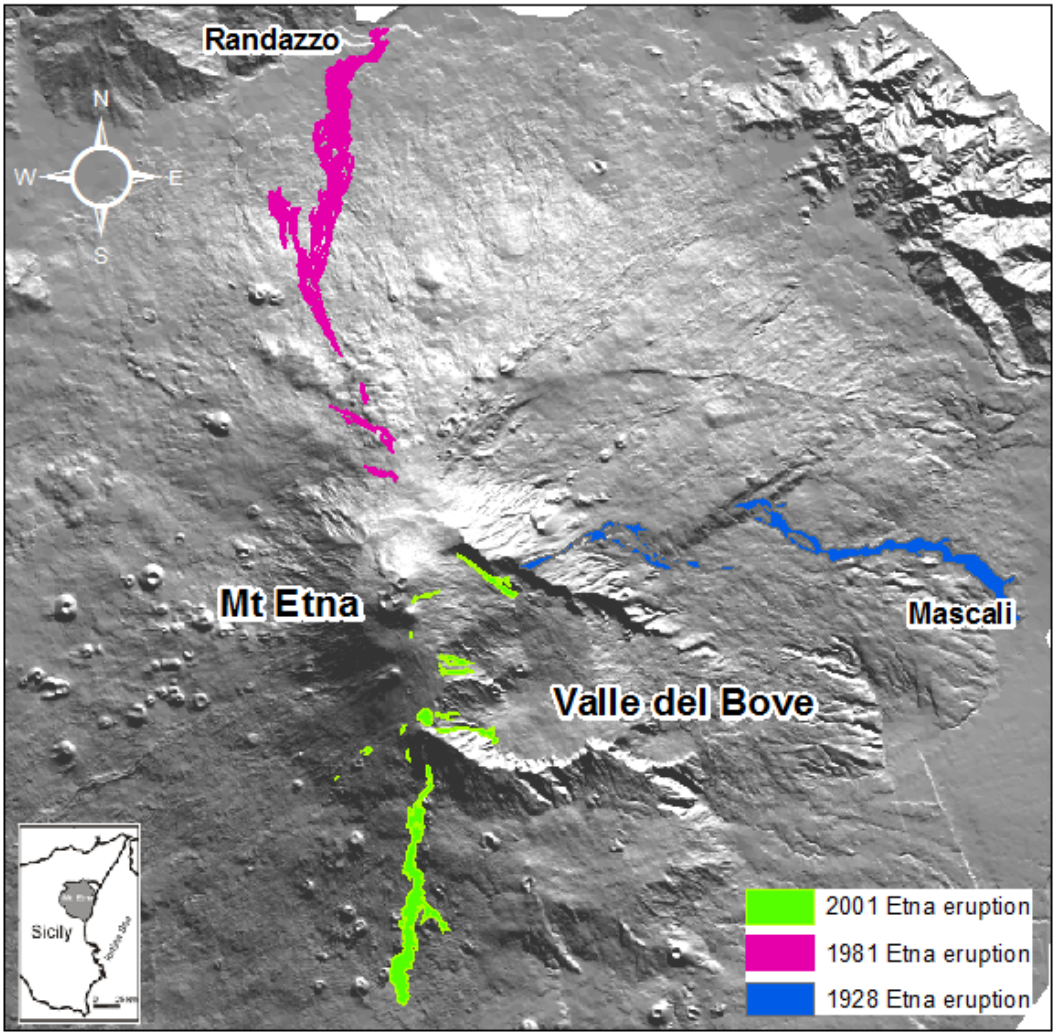
Randazzo
N
W
E
S
Mt Etna
Mascali
Valle del Bove
Sicily
2001 Etna eruption
1981 Etna eruption
1928 Etna eruption

Figure 2.1

2.1 Lava effusion rate definition

In this chapter we give report some definition of parameter that quantify the output rate of an eruption. Harris et al.([40]) defines "Instantaneous Effusion Rate" (IER) like the volume flux of erupted lava that is feeding flow at any particular point in time. Such measurements, if made repeatedly over a short period of time, are useful in defining short-lived surges in the lava flux developing over seconds to minutes. "Time Averaged Discharge Rates" (TADR) consider volume fluxes averaged over a given time period. This is typically obtained by measuring the volume emplaced and usually includes both the effusive and the explosive products, and dividing it by the duration to give volume flux over that interval. "Eruption Rate" (ER) is defined as the total volume of the lava emplaced since the beginning of the eruption divided by the time since the eruption began. To study the past flank events the eruption rate is not useful because it smooths any variation in the effusion rate, while the instantaneous effusion rate measurements made during a short-lived surge in effusion are not representative of the typical flux for the longer time period. Furthermore, the measurement of instantaneous effusion rate requires field measures to calculate the mean velocity at which lava flows through the cross - sectional area of the channel. These data are not available for past flank eruptions. Using the TADR the advantage of this measurement over instantaneous effusion rate is that short-term variations, caused by short-lived changes in measurement conditions, or bias introduced by the time of measurement can be minimized, allowing the identification of a general trend of the eruption. Furthermore, using the volumetric approach described below, it was possible estimate the TADR for past flank eruptions by measuring the change in volume of a lava flow over a known period of time.

2.2 Historical flank eruption reconstruction: the quantitative approach for TADR trend estimation

In this work in order to quantify lava emplacement processes and in particular the evolution of the TADR, a volumetric approach was applied. This approach

consists in:

- Delimiting the final lava flow field using orthophotos or historical maps;
- Obtaining the pre and post topography using photogrammetry or digitizing historical maps;
- Estimation of the final volumes by subtraction of the pre- and post eruption Digital Elevation Model (DEM);
- Reconstruction of the temporal evolution of the lava flow field;
- Obtaining the Time Average Discharge Rate (TADR) trend.

2.2.1 DEM extraction

The DEMs were extracted using digital photogrammetry or historical cartography. The DEMs extracted from photogrammetric data were obtained using a digital photogrammetric workstation through a semi-automatic procedure ([2]). Stereo pairs, acquired before and after the eruption, form the photogrammetric blocks covering the whole area of interest. Ground Control Point (GCPs) were identified and measured on recent high resolution DEM and orthophotos in areas not covered by lava flows. GCPs were used for the orientation procedure in conjunction with a set of Photographic Control Points (PCPs) measured on photogrammetric data set ([3]).
For the oldest eruptions (such as the 1928) historical maps were acquired. To extract DEMs from these maps, it was necessary to digitize the contour lines from which the DEMs were created. In this case the TIN (Triangular Irregular Network) method, based on Delaunay triangulation, was utilized to interpolate elevation data. The TIN method partitions a surface into a set of contiguous, non-overlapping triangles. A height value is recorded for each triangle node.

2.2.2 DEM quality assessment

To evaluate the method's accuracy and check DEM's the co-registration a detailed comparison of the pre and post eruption DEMs is carried out on the whole map area in order . Elevation residuals outside the lava flow margin (terrain

residuals) are used to assess horizontal and vertical mis-alignments between the pre and post eruption DEMs. To estimate DEM quality using external data, in some cases GPS surveys are carried out on selected test areas. GPS control points, distributed both inside and outside the lava flow area are measured and the elevation of each GPS point are compared with that extracted at the same location from the pre- and post-eruption DEMs.

2.2.3 Volume estimation

The vertical difference inside the area covered by the lava flow are used to estimate the volume of the lava flow and the thickness's distribution. Portions of the lava flows are remodelled as a consequence of rebuilding of the area, the flow volume cannot be evaluated as a straightforward comparison between the two DEMs. Field surveys permit the estimation of the average thickness of adjacent flow portions and thus to evaluate the corrections that should be applied to the lava thickness measurement. The temporal evolution of the lava flow field, together with the position of the lava flow fronts at different times, are reconstructed taking into account various data sources including photos from a helicopter or field surveys, scientific literature, scientific reports and detailed chronicles reported on local newspapers. The temporal evolutions are used in order to estimate the volume emplaced over the given time interval to obtain the TADR trend of the eruption. In order to estimate the volumes (V) of the lava flows we compared the pre- and post-eruption DEM (2.1):

$$V = \sum_{ij} \Delta x^2 \cdot \Delta z_{ij} \tag{2.1}$$

where Δx is the linear dimension of the square cells and Δz_{ij} is the height variation between pre and post eruption DEMs that represents the lava thickness. Since Δx is constant V can also be evaluated by (2.2):

$$V = n_{tot} \cdot \Delta x^2 \cdot \overline{\Delta z} \tag{2.2}$$

where n_i is the number of cells inside the lava flow limits while n_p is the number of cells covering the flow perimeter and $\overline{\Delta z}$ is the average lava thickness. The variance associated with the lava volume is calculated by applying the variance

propagation law to (2.2):

$$\begin{aligned}\sigma_v^2 &= \left(\frac{\delta V}{\delta(\overline{\Delta z})}\right)^2 \cdot (\sigma_{\overline{\Delta z}})^2 + \left(\frac{\delta V}{\delta(\Delta x)}\right)^2 \cdot (\sigma_{\Delta x})^2 \\ &= \left((n_i + n_p) \cdot \Delta x^2\right)^2 \cdot (\sigma_{\overline{\Delta z}})^2 + \Big[\left(2 \cdot n_p \cdot \Delta x \overline{\Delta z}\right) \\ &\quad + \left(2 \cdot n_i \Delta x \overline{\Delta z}\right) + 8 n_i n_p \Delta x^2 \cdot \left(\overleftarrow{\Delta z}\right)\Big] \cdot (\sigma_{\Delta x})^2 \end{aligned} \tag{2.3}$$

where $\sigma_{\overline{\Delta z}}$ is the vertical accuracy of the lava thickness evaluated as the standard deviation of the terrain residuals, that is the height variations between the two DEMs evaluated in unchanged areas, while $\sigma_{\Delta x}$ is a horizontal accuracy evaluated as twice the orthophoto resolution. Since the horizontal error is only due to the drawing of the lava flow field limits, the cells inside the lava flow can be considered as having zero error, $n_i \cdot \sigma_{\Delta x} = 0$, therefore the third and fourth terms of equation (2.3) are equal to zero and the standard deviation of the volume V can be obtained as follows:

$$\sigma_V = \sqrt[2]{\left(n_{tot} \cdot \Delta x^2\right)^2 \cdot (\sigma_{\overline{\Delta z}})^2 + \left(2 \cdot n_p \Delta x \cdot \overline{\Delta z}\right)^2 \cdot (\sigma_{\Delta x})^2} \tag{2.4}$$

This procedure for estimating the volume uncertainties does not take into account the systematic errors since the co-registration procedure described before should have reduced the biases between the two DEMs.

2.3 The 2001 Etna eruption

2.3.1 Eruption chronology

The 2001 eruption started on 17th July with the opening of an eruptive fissure at the base of South East Crater (SEC) on the volcano summit. During the subsequent days other six fissures on the southern and northeastern flanks of the volcano, from the summit down to 2100 m a.s.l, opened ([20])(fig. 2.2). The

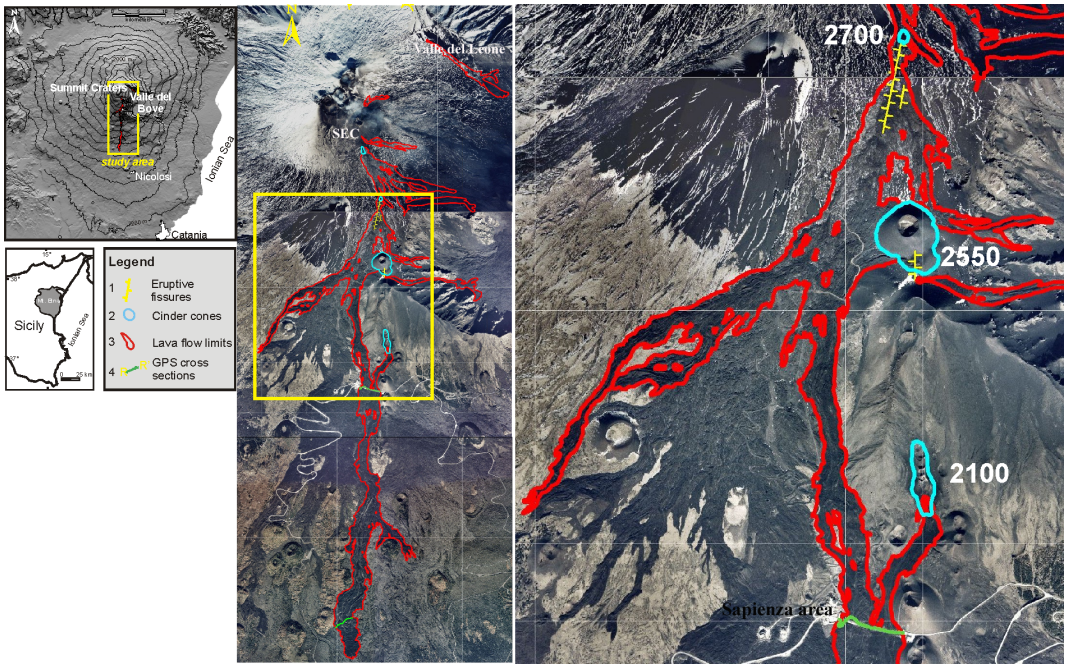

Figure 2.2: The left figure locates Mt. Etna in the eastern part of Sicily and the 2001 eruption on the volcano edifice. The central figure shows lava flows limits (red), eruptive fissures (yellow) and scoria cones (light blue) of the whole lava field emplaced during July-August 2001 defined on the post eruption orthophotos. The right figure reports the lava flows, from the 2700 m and 2550 m a.s.l. vents, involved in the building of barriers to protect the Sapienza area.

upper vents were located one at the foot of the SEC, two on the flanks of the South-East cone, one on the south flank between 2780 and 2640 m a.s.l. (fracture 2700 m) and one in "Valle del Leone", on the northern flank. The vents at 2700 m a.s.l. and 2550 m a.s.l. fed lava flows from 18 to 27 July and 26th to 31st July, respectively. In this work we quantitatively reconstruct just these two lava

flows that caused damages and threatened some important tourist facilities and infrastructures which were protected by thirteen earthen barriers ([6]).The first five barriers (B1, B2, B3, B4, and B5) aimed to slow down the lava flow descending towards Rifugio Sapienza from the 2700 m vent. Seven barriers (C1, C2, C3, C4, B6, B7, and B8) were built to control the advancement of the 2550 m lava flow. A barrier (A) was also erected to protect the facilities near "Mt. Silvestri" from the lava flowing from the 2100 m vent. The lava totally or partially surmounted all the barriers, with the exception of the southernmost part of the C4 barrier which was fundamental in diverting the flow because it prevented the lava from invading the built-up part of the "Sapienza area" ([6])(fig.2.3).

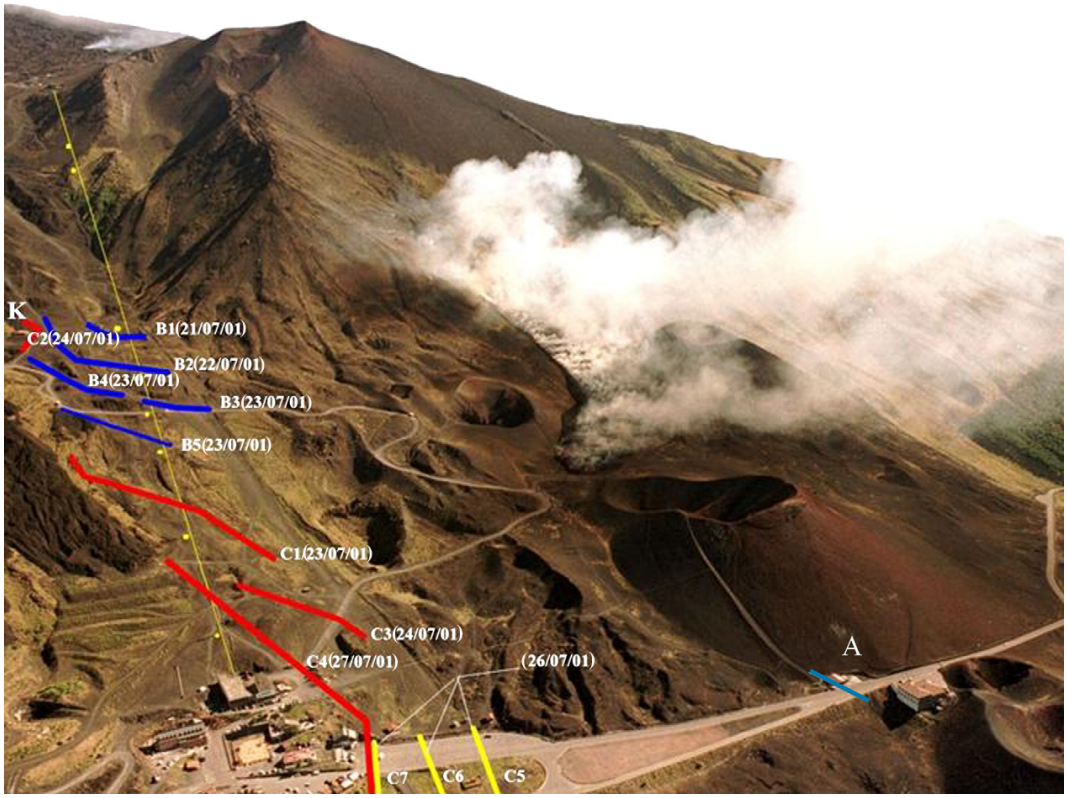

Figure 2.3: Photograph of the Montagnola, Silvestri, Sapienza zone on 17 July. The location of the barriers are indicated together with the data of their construction (in bracket)(Modified from [6])

Day	Helicopter photo (vent 2700 m)	Helicopter photo (vent 2550 m)
18 July	Yes	No lava flow
19 July	Yes	No lava flow
20 July	Yes	Yes
21 July	Not useful	Not useful
22 July	Yes	Yes
23 July	Not useful	Not useful
24 July	Not useful	Not useful
25 July	Yes	Yes
26 July	Yes	Yes
27 July	Partially visible	Not useful
28 July	No active flow	Yes
29 July	No active flow	Yes
30 July	No active flow	Partially visible
31 July	No active flow	Partially visible

Table 2.1: List of the helicopter photos available for the flows from the 2700 m a.s.l. fissure and 2550 m a.s.l. vent.

2.3.2 Quantitative reconstruction and TADR trend estimation

The reconstruction of the lava flows evolution was based on the analysis of helicopter photos taken during the event and post eruption orthophoto. Helicopter surveys were carried out almost every day during the 2001 eruption for surveillance purpose collecting digital images that allowed to reconstruct the lava flows evolution. Daily maps were drawn on the basis of the photo availability, quality and usefulness (tab.2.1). Information on flow front position were also obtained from the daily "Istituto Nazionale di Geofisica e Vulcanologia (INGV)" reports and utilized as an additional check. Figure 2.4 shows the temporal evolution of the 2700 m and 2550 m a.s.l. lava flows between 18 to 31 July. On the basis of the daily maps the flow emplacement can be divided in three phases: the 1st phase (18 - 22 July) involved only lava flow from 2700 m a.s.l. fissure; the 2nd and 3rd phase (25 - 27 July and 27 - 31 July) show the evolution of both flows. Since the 2550 m vent emitted a lava flow that partially covered the 2700 m lava flow. The pre-eruption DEM was obtained interpolating contour lines and eleva-

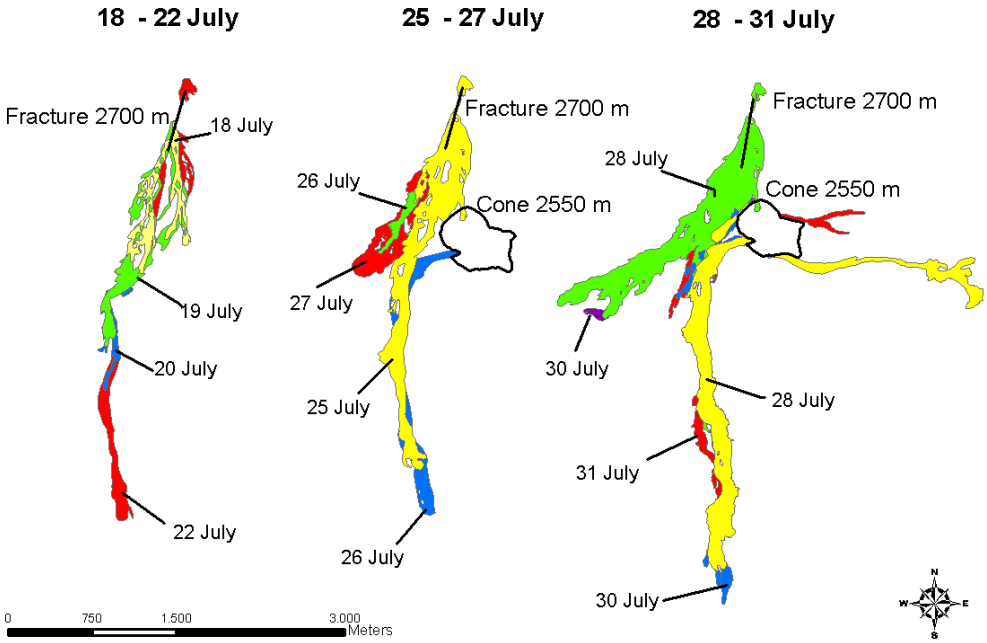

Figure 2.4: Temporal evolution of the lava flows from the 2700 m and 2550 m a.s.l. vents between 18 and 22 July, 25 and 27 July, and 28 and 31 July.

tion points of the 1:10.000 vector map issued by the PRC (Provincia Regionale di Catania) from an aerial survey performed in 1998. The post eruption DEM was interpolated from the 2001 vector map of PRC extracted from the 3 December 2001 aerial survey. The barriers built during the eruption were superimposed on the pre eruption topography. The lava thickness of the flow was obtained differencing the post-eruption and the pre-eruption DEMs(2.5). After the 26th July, the flow

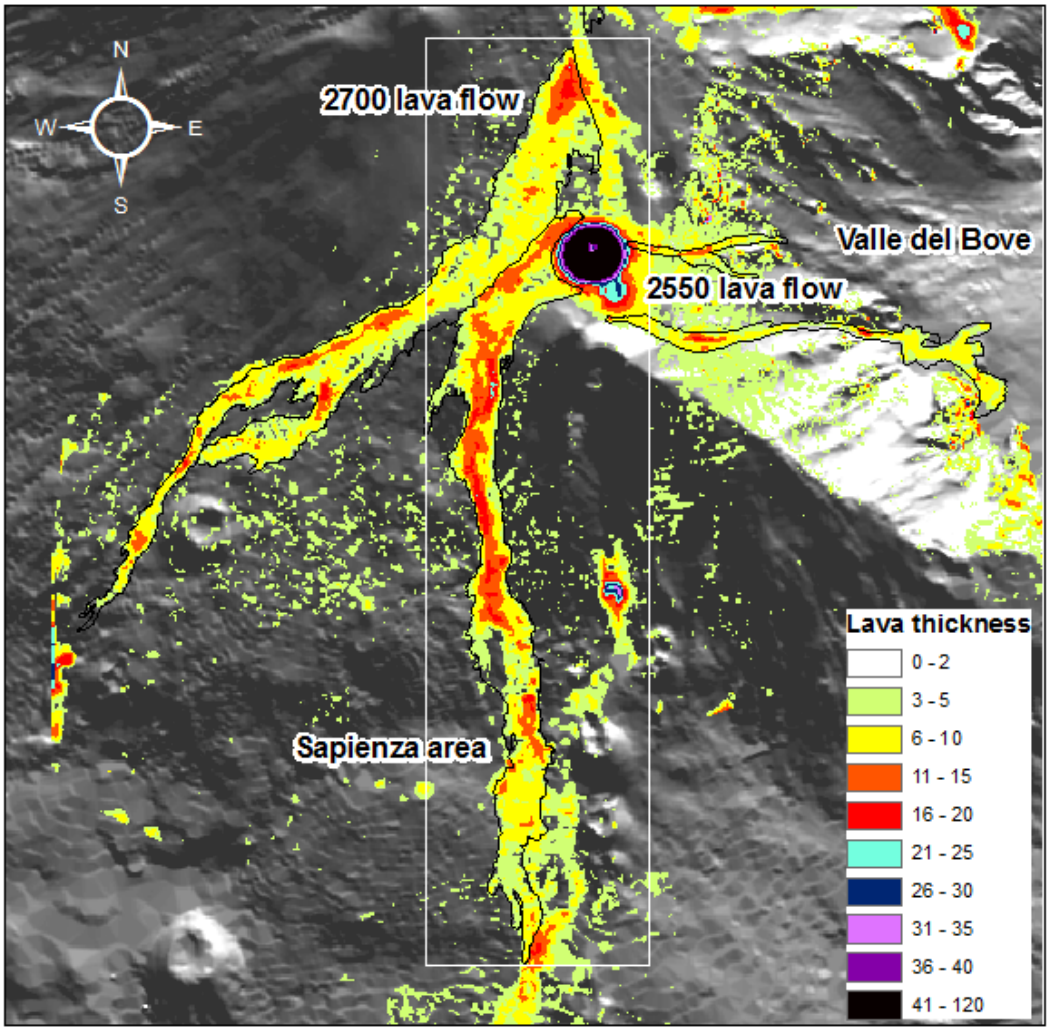

Figure 2.5: Lava thickness of 2700 and 2550 lava flow of the 2001 Etna eruption.

from the 2700 m vent was partially buried by that of the 2550 m vent, thus it was more difficult to define the daily limits of the 2550 m flow field and to estimate the

thickness's of both flows. In this case the estimation of the thickness was based on a morphological analysis of the pre and post eruption topography. In order to reconstruct the daily average thickness's, the area covered by the two flows was divided into three zones: the first was the one covered only by lava emitted from the 2700 m vent (ZONE 1), the second zone was covered by lava from both the 2700 m and 2550 m vents (ZONE 2), and finally, the third zone was covered only by lava from the 2550 m vent (ZONE 3) (2.6). The final lava thickness's were evaluated as the difference between the Z value of a point in the post eruption DEM and the corresponding point on the pre-eruption DEM for the ZONE 1 and 3. To study the lava emplacement in the ZONE 2 cross - sections were drown on the lava field. From a morphological analysis of these cross - sections thickness's of the two lava flows were estimated. The cumulated volumes of the two flows were then calculated at every survey dates obtaining the TADR trends showed in figure 2.7.

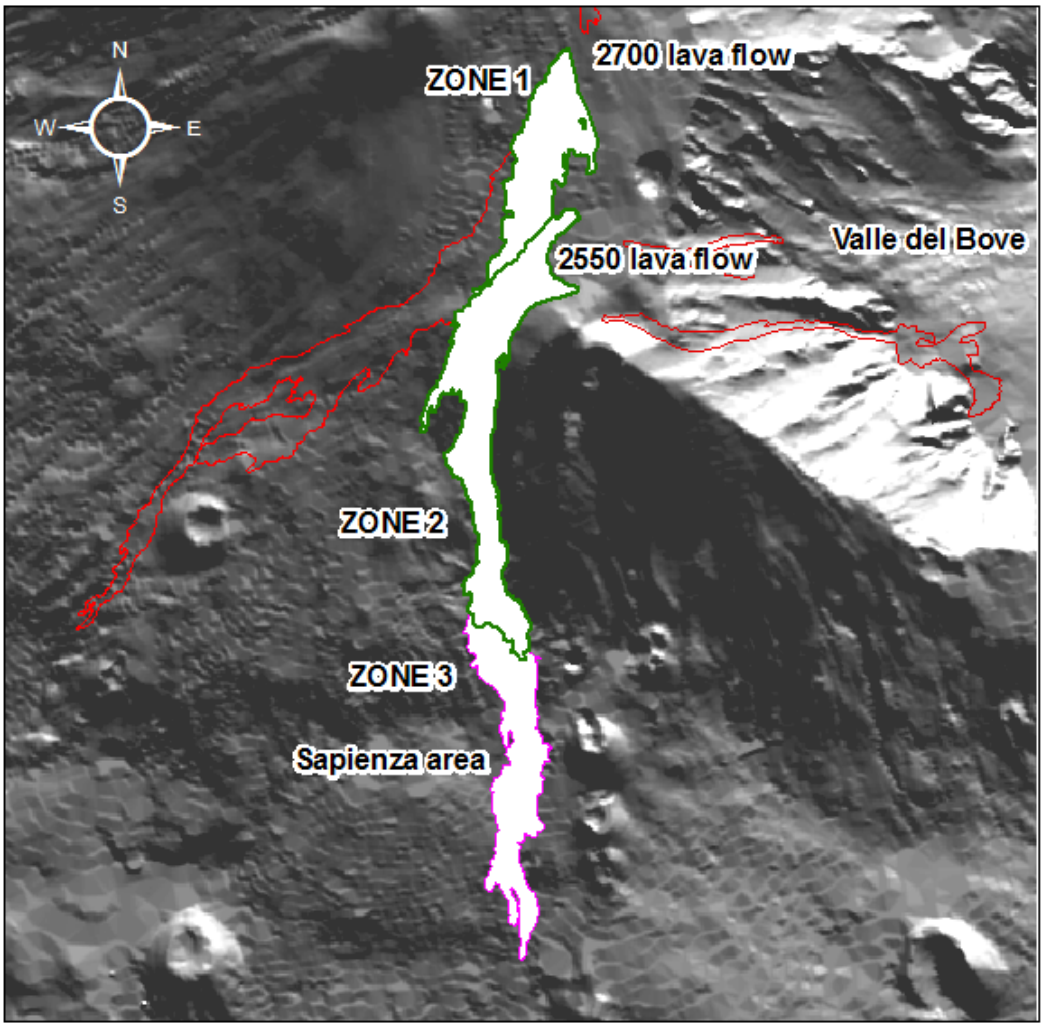

Figure 2.6: The area covered by 2700 and 2550 lava flows were divided into three zones: the first was the one covered only by lava emitted from the 2700 m vent (ZONE 1), the second zone was covered by lava from both the 2700 m and 2550 m vents (ZONE 2), the third zone was covered only by lava from the 2550 m vent (ZONE 3)

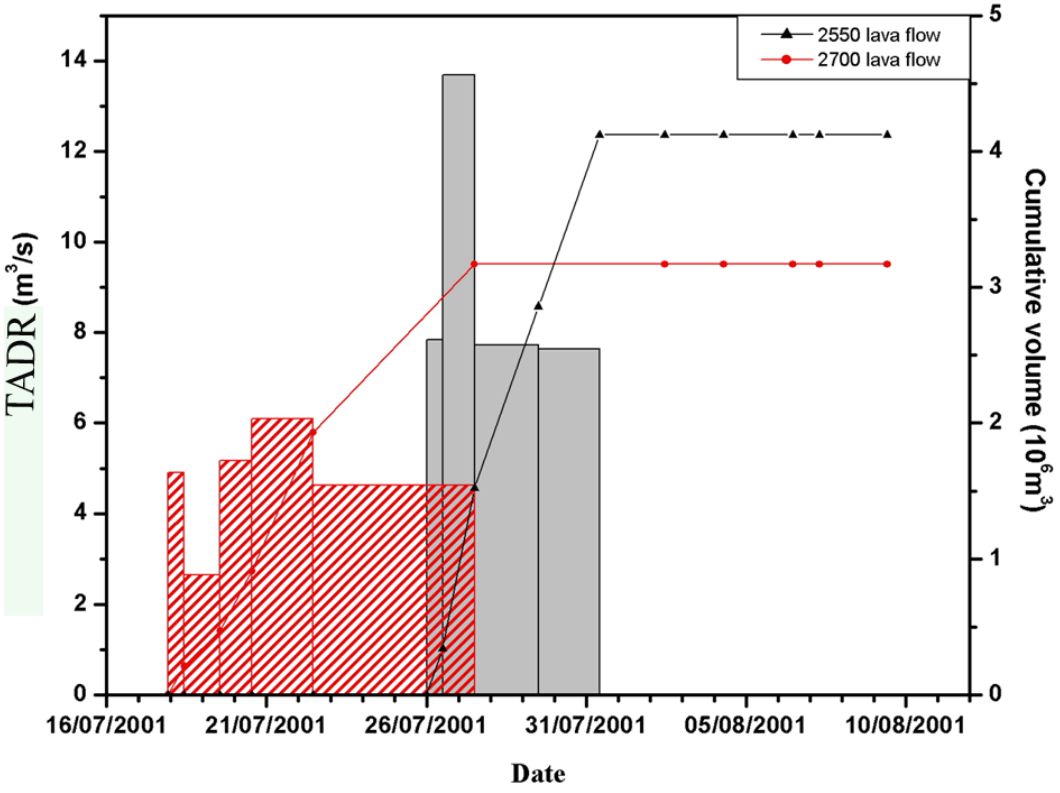

Figure 2.7: Time average discharge rate (TADR) of the 2700 and 2550 lava flows (2001 Etna eruption).

2.4 The 1981 Etna eruption

2.4.1 Eruption chronology

The temporal evolution of the 1981 Etna lava flow field, including the positions of the lava flow fronts at different times, was reconstructed from scientific documents ([22];[62];[37]), scientific reports ([78];[45]) and detailed chronicles reported in local newspapers. After the end of the 1979 flank eruption, vigorous summital activity resumed at Etna in April 1980. The volcano was characterized by both discontinuous strombolian activity and lava fountain episodes at the South East Crater (SEC), as well as at Voragine (VOR) and Bocca Nuova (BN) summit craters (2.8). On 1st September, the activity shifted to the North East Crater (NEC) forming a strong lava fountain eruptive episode characterized by the emission of two lava flows 3-4 km long. Early the next day the activity waned but another similar paroxysmal episode occurred at the same crater (NEC) on 6th September and was characterized by both violent explosive activity and lava overflow for about 10 hours. Strong strombolian activity resumed again on 5th February at the same crater and lava poured out from its base forming three lobes that travelled about 2 km up to 7th February. Ash emissions from the VOR were noticed both at the end of the NEC activity and during the last days of the month, when the SEC also showed similar activity. During the first half of March, ash emission together with ejection of spatter were observed from the VOR and, sporadically, from the NEC ([78]). The 1981 flank eruption was preceded by a swarm of local earthquakes which started on the morning of 16th 110 March. Figure 2.8 show a map of the northern flank of the volcano where the eruptive fissures, the evolution of the lava flows as well as the roads and sites in the following discussion are cited. On 17th 111 March at 1:37 p.m. (local time) a NS trending eruptive fissure (F1a), opened at 2595 m a.s.l. (tab.2.2).

The F1a initial activity was characterized by lava fountaining, at the same time a sudden emission of ash from the BN was observed. From 1:37 p.m. to 5:21 p.m. three eruptive fissures opened downslope, two (F1b and F1d) followed a NW trend, while one (F1c) showed a WNW strike ([78]). Short-lived lava flows were emitted along the F1 fissures in correspondence to the four distinct segments (F1a, F1b, F1c, and F1d). At 6:55 p.m. a new eruptive fissure (F2a) opened to the East of Mt

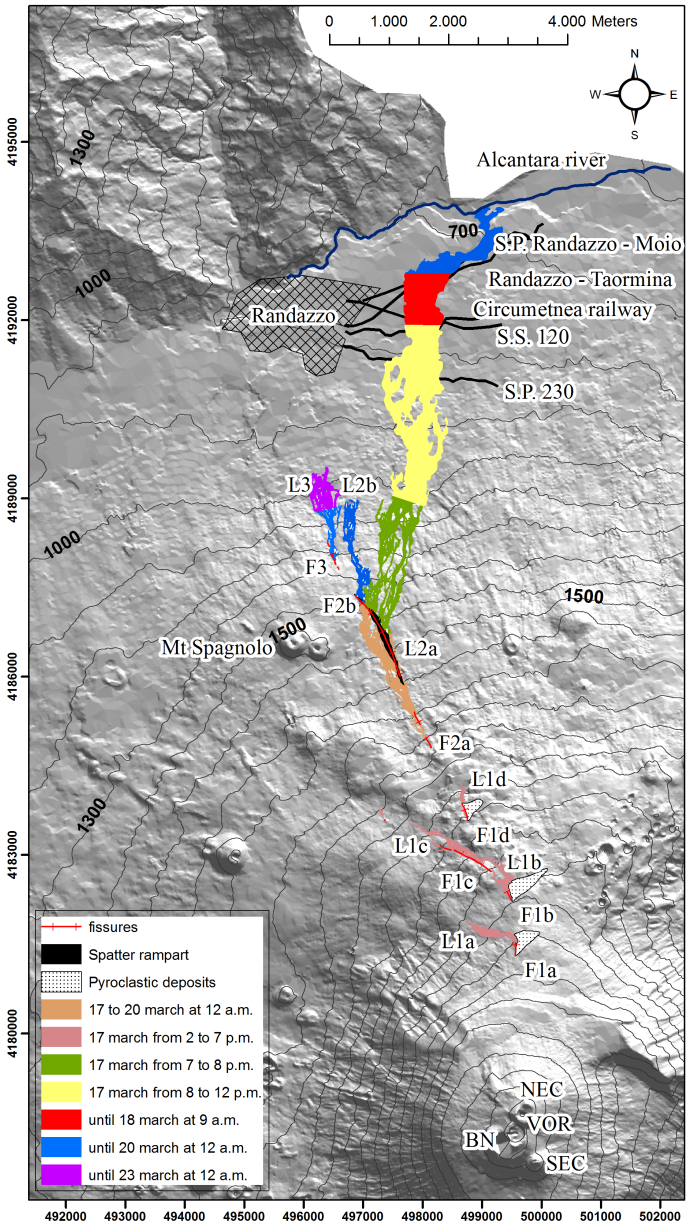

Figure 2.8: Fissure system and temporal evolution of the lava field of the 1981 Etna eruption. The infrastructures covered by the lava flows as well as Randazzo towns, the Alcantara river and the summit craters: Bocca Nuova (BN), Voragine (VOR), South East Crater (SEC) and North East Crater (NEC) are also indicated.

Opening time	**Fissure name**	**Fissure trend** (°)	**Length** (m)
17 March from 1.37 p.m.	F1a	4	230
	F1b	332	190
	F1c	300	944
	F1d	340	314
17 March from 6.55 p.m.	F2a	334	1760
18 March from 10.00 p.m.	F2b	330	240
	F3	335	363

Table 2.2: Opening time, name, trend and length of the 1981 Etna eruptive fissures

Spagnolo between 1800 and 1350 m a.s.l. From the lowermost section of this fissure, between 1400 and 1350 m a.s.l., a large lava flow (L2a) started. Between 8:00 p.m. and midnight of 17th March this flow rapidly inundated the "Circumetnea railway" and the main road (S.S. 120), reaching an elevation of 730 m a.s.l. at about 5 km from the vent. By 18th March at 9:00 a.m. the main lava flow had advanced an additional 1 km, covering the railway "Taormina-Randazzo" and the main road ("S.P. Randazzo-Moio"). At 10:00 p.m. on the same day, additional eruptive fissures (F2b and F3) opened at lower altitudes (between 1350 and 1310 m a.s.l. and between 1227 and 1117 m a.s.l., respectively) producing lava flows (L2b and L3) that slowly advanced towards "Randazzo". The L2a flow slowed reaching the "Alcantara" riverbed (600 m a.s.l.)at 11:00 a.m. on 19th March. During this day the L2a flow remained confined within the "Alcantara" riverbed and continued to be fed, thickening its frontal portion but not further by advancing. On midday of 20th March the lava outpouring from F2a stopped and the main lava flow L2a reached its final length of 10 km. At the same time a small spatter cone built up above the F3 emission point as a consequence of a weak explosive activity that accompanied the slow advancing of the only active lava flow (L3). The eruptive activity from F3 fissure continued with variable intensity until the end of 23rd March when the lava front stopped at 926 m a.s.l.

2.4.2 Quantitative reconstruction and TADR trend estimation

The pre eruption DEM was extracted from a photogrammetric dataset acquired during an aerial survey performed in 1978 by Rossi Brescia S.r.l. at a flight altitude of 3000 m (scale 1:20.000). Aerial photos collected during a photogrammetric survey performed in 2004 were processed to extract post eruption topography. In order to obtain a complete coverage of the lava field below 2000 m a.s.l., it was necessary to integrate the 2004 DEM with a DEM obtained by interpolating a 1:10.000 contour map updated to 1999 ([20]). In order to assess the accuracy of the 1978 and 2004 DEMs, GPS surveys were carried out in 2008 and in 2009 on selected test areas. The comparison evidenced an average difference of about 0.3 m for the post eruption DEM and of about 0.9 m for the pre eruption DEM. After the co-registration of two DEMs the vertical differences were considered only inside the flow limits, excluding the internal areas not covered by new lava, and enabled the preparation of the residual map, which shows the distribution of lava thicknesses at the end of the eruption (2.9). Unfortunately, the simple difference between the two surfaces does not provide a correct estimate of the volume because the DEM are not exactly corresponding to the situation before and after the event. The upper portion of the L2a flow destroyed mature and dense forests thus the height of the vegetation should be considered in the volume calculation. Similarly, the lower portion of the L2a was in part modified as a consequence of refurbishment of the urbanized area. Field measurements were performed for measuring, on the unchanged areas the lava thickness to be assigned to the adjacent modified zones. The volumetric approach was applied to evaluating the volume of both the lava and the pyroclastic products emplaced during the 1981 Etna eruption from each eruptive fissure (tab.2.3). The obtained total volume is 22.75 $10^6 m^3$ to which was assigned a relative error of 24% estimated following the procedure in paragraph 2.2. The total volume of the lava emplaced divided by the total time of the eruption (142 h) allowed us to calculate an eruption rate of 44.5 m^3/s. The temporal evolutions of the flows were reconstructed in order to estimate the discharge rate trend during the eruption. This reconstruction was based on the information on front position, recovered from the event chronologies, that allowed mapping the lava advancement (fig. 2.8). Nevertheless, no sufficient

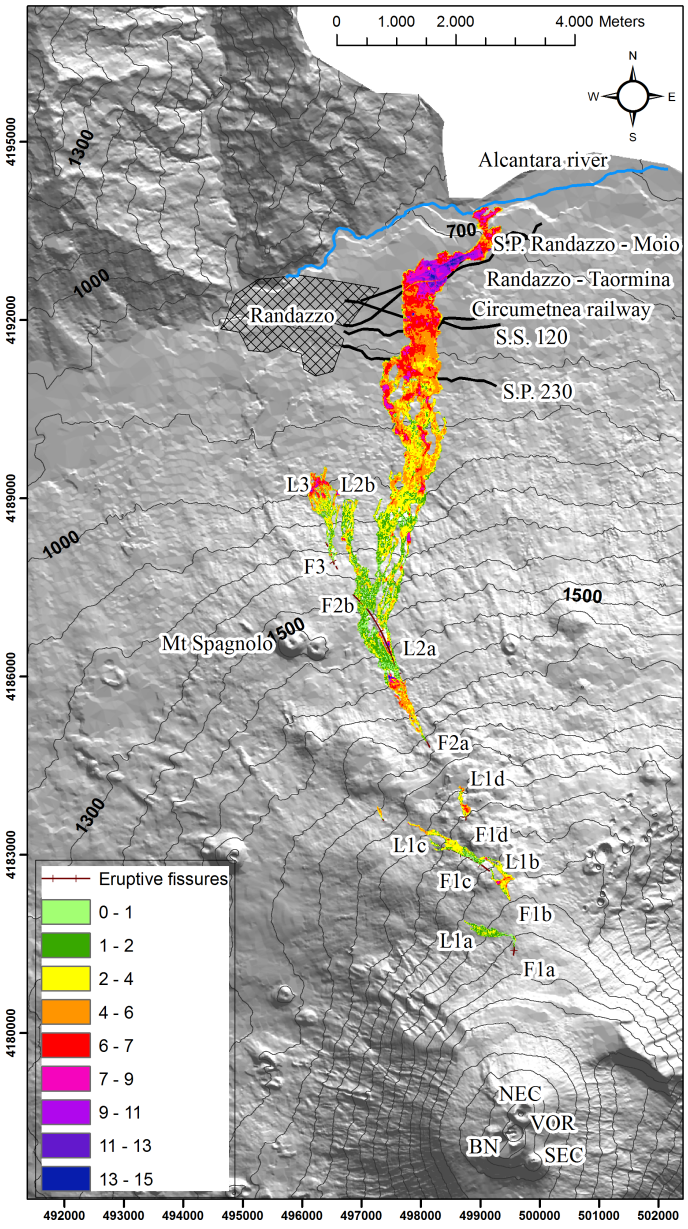

Figure 2.9: Distribution of the final lava thicknesses of the seven flows composing the 1981 lava field as evaluated from the comparison of the pre and post-eruption DEMs.

Eruption deposits	Length (Km)	Area ($10^6 m^2$)	Volume ($10^6 m^3$)
L1a	1	0.1	0.05
L1b	0.9	0.1	0.38
L1c	1.5	0.15	0.5
L1d	0.5	0.4	0.15
P1	-	0.28	0.54
L2a	10	3.97	18.80
P2a	-	0.1	0.55
L2b	1.7	0.23	0.48
L3	1.6	0.34	1.30

Table 2.3: Length, area and volume of the 1981 Etna eruption deposits. In the column eruption deposits L, P1 and P2a indicate lava flows, pyroclastic fall deposit and spatter ramparts, respectively.

data were available for defining the lava flow limits at regular time intervals. The partial and cumulative volumes of L2a, L2b and L3 were reconstructed by splitting the final lava thickness through the flow field limits drown at each time step (2.8) and measuring the volume only inside the corresponding area. The temporal evolution of the eruption and the analysis of final lava thickness's both indicate that the flows emplaced mostly as single units and that the super-imposed lava units can be considered negligible, except for the L2a lava fronts which reached the Alcantara riverbed. The volume of the spatter rampart ($0.55 \cdot 10^6 m^3$) built up above F2a was included and proportionally distributed, with respect to the time, in the volume of the corresponding lava flow.

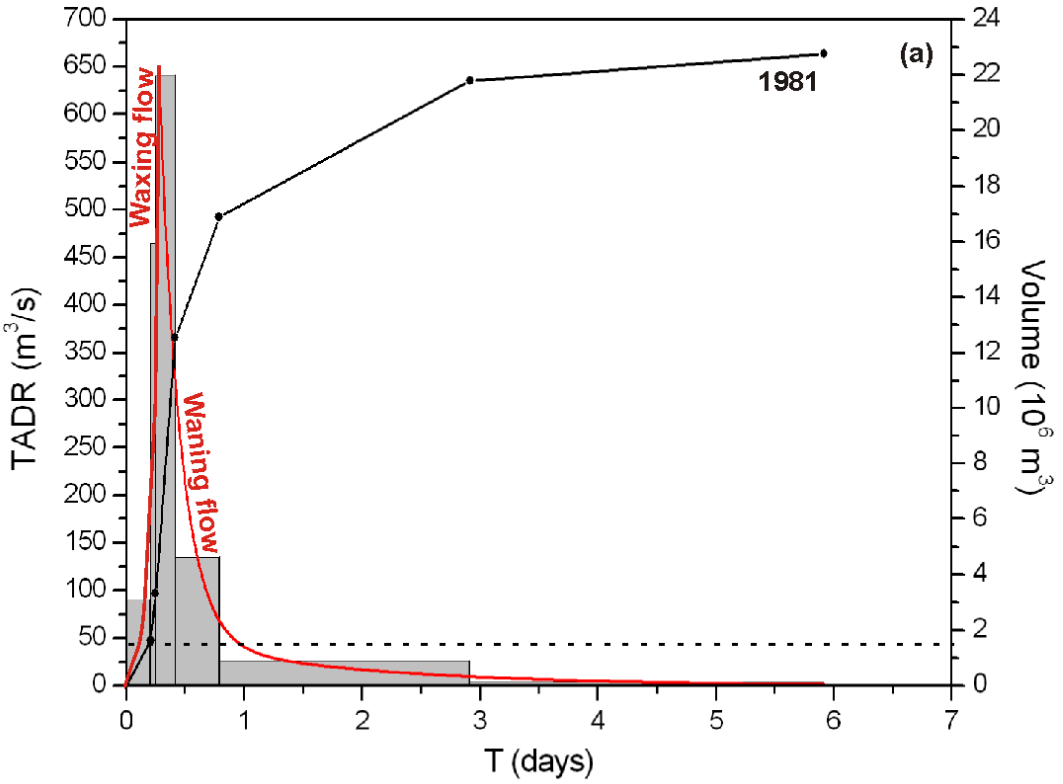

Figure 2.10: Time averaged discharge rates (TADR), on the left axis, and cumulative volumes, on the right axis, of the 1981 eruption (a). Red lines shows the interpolated discharge rate trends (using an exponential fit) that illustrate the waxing and waning phases. Dashed line shows the eruption rate value.

2.5 The 1928 Etna eruption

2.5.1 Eruptive chronology

The eruption began at 4.30 pm (local time) on 2nd November 1928 with an explosion from the NEC. An ash-laden cloud rose over 1.000 m. This was followed by frequent explosions, about every minute lasting an hour until 6 pm. A rift opened at 2.600 m in the "Valle del Leone" forming a fissure of 150 m length ([43]). A small short-lived lava flow, about 500 m long and 200 m wide, outpoured from this fissure. This first phase of the eruption was later totally covered by other products and it was not considered in this reconstruction. A second fissure opened on the 3 November at 3.30 a.m. at the NEC between 2200 m and 1550 m. A lava flow fed by this fissure covered the "Cerrita" and "Cubania" forests and flowed around the town of "Sant'Alfio" without causing damage to the town. At 12 points along this fissure, vents developed and voluminous lava streams poured out from the lower regions of the fissure. The activity ended on 4th November([27])(fig. 2.11) leaving a lava flow field extending for about 3.5 km down to an altitude of 1000 m. At 9 pm of the same day following earth tremors a third fissure opened along "Ripa della Naca" fault system and erupting lava at high effusion rates from a series of small vents at 1200 m. The lava flow, about 160 m wide, divided into three branches, directed toward Mascali town that was just 5 Km distant from the vents. At 11 pm the lava flow reached and covered houses at "Pietrafucile" and "Costa Sovara". During the night the lava coming out from the fissure produces short explosion. Between 5th and 6th November there was a high discharge rate of lava and the flow advanced rapidly downslope. On 6th November at 5 am the lava flow advancing at a speed of 2 m/min reached a length of about 6.5 km and the Circumetnea rail was reached. At 7 am the Road between "Nunziata - Piedimonte" was cut ([32]). During the same day at the 6 pm the flow reached the first house of Mascali. Most of Mascali was destroyed during the 7th November, but the rate of advance of the lava slowed and the main railway line, about one km downslope, was not cut until the 11th November. The flow front finally stopped on 16th November at an altitude of about 25 m after having reached the first houses of "Carrabba". The eruption ended on 20 November 1928 ([24]).

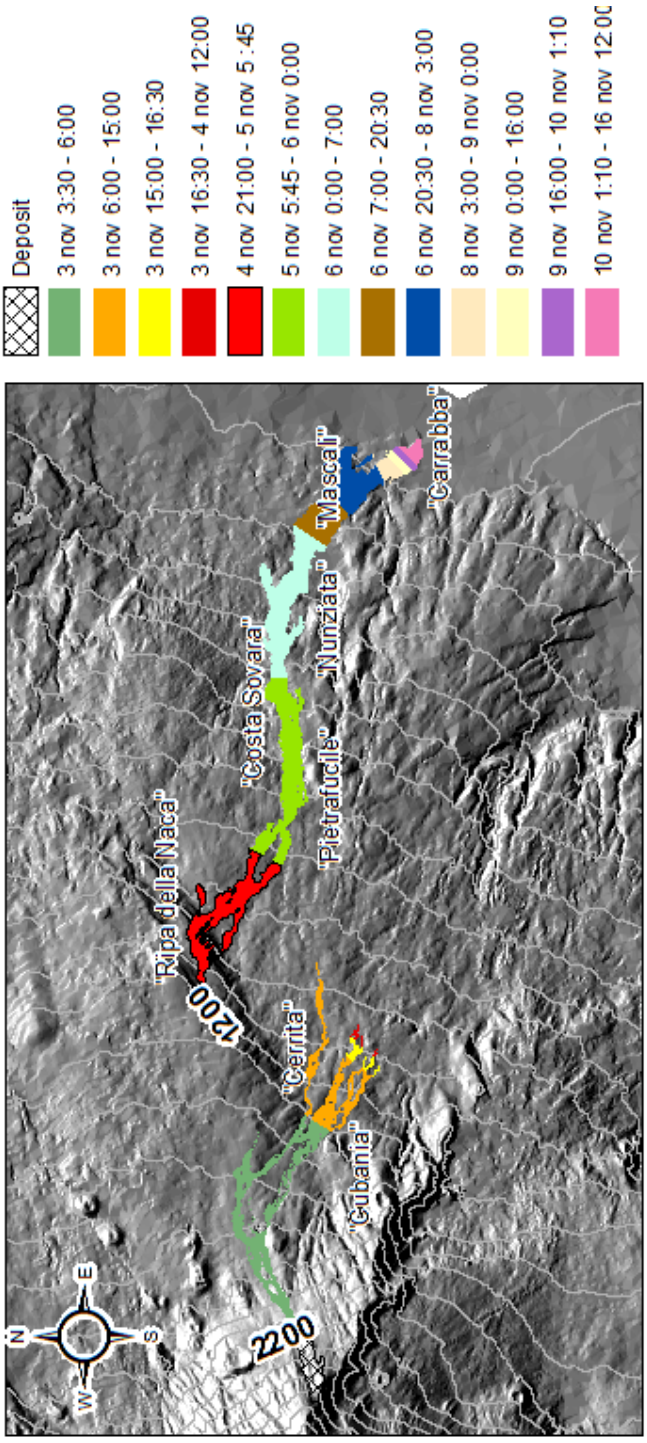

Figure 2.11: Temporal evolution of the lava field of the 1928 Etna eruption.

2.5.2 Quantitative reconstruction and TADR trend estimation

A 1877 (scale 1:50000), 1868 (1:30000) and 1938 (scale 1:25000) historical maps from the IGMI (Istituto Geografico Militare) were used to reconstruct the pre eruption and post eruption topography: Contour lines as interval of 10 m were digitized. The TIN (Triangular Irregular Network) method was used to interpolate elevation data and obtained a DEM. DEMs processing in a grid format with size 10 m ([59]) were used to reconstruct the pre- and post- eruption topographies.
Furthermore, another a post eruption DEM was obtained processing photogrammetric photos acquired during an aerial survey performed in 1967 by IGMI at a flight altitude of 4900 m (scale 1:32.000).
Original lava thickness's were calculated by subtracting the pre and post eruption DEMs. The 1928 lava field has been modified in many areas in order to rebuild the town of Mascali or to quarry the basalt. Field surveys were performed inside the quarries for measuring, through a laser binoculars, the lava thickness along the exposed walls. The measured thickness's were assigned to the surrounding modified areas obtaining the final lava thickness map (fig. 2.12). The eruption emitted a total lava volume of $65 \cdot 10^6 m^3$ ([24]). In order to reconstruct the partial volumes at different times the lava flow thickness was obtained cut at the front positions derived from chronology. In figure 2.13 the TADR for the lava flows from the 2200 m and 1200 m fissures are shown: the upper fissure the trend was characterized by the presence of an high peak of discharge rate caused by explosive activity while for the second fissure the trend is quite regular because the 1200 m lava flow is a result of degassed magma.The different behaviour is probably linked to the characteristic of the source that feeds the two flows and need further investigation.

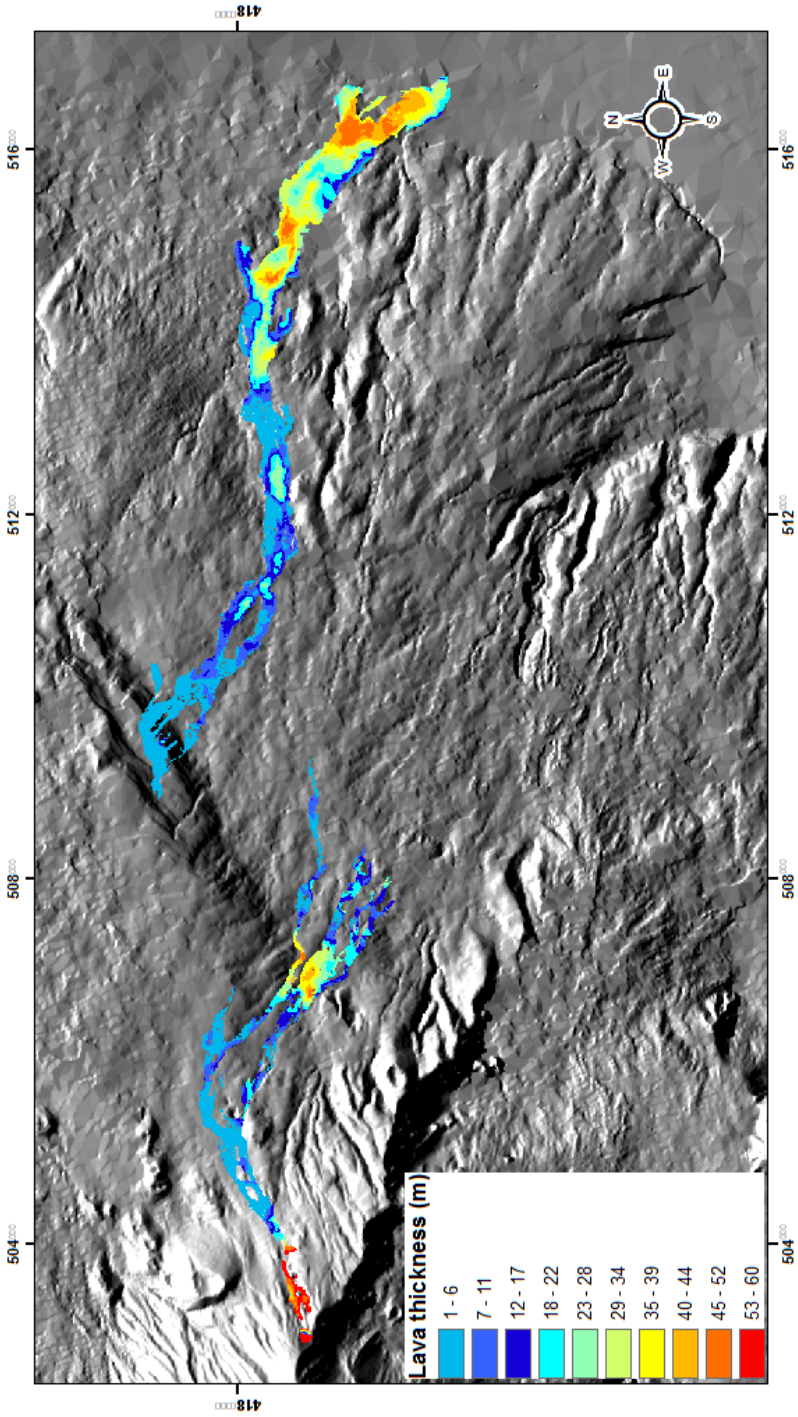

Figure 2.12: Lava thickness map of the 1928 Etna eurption

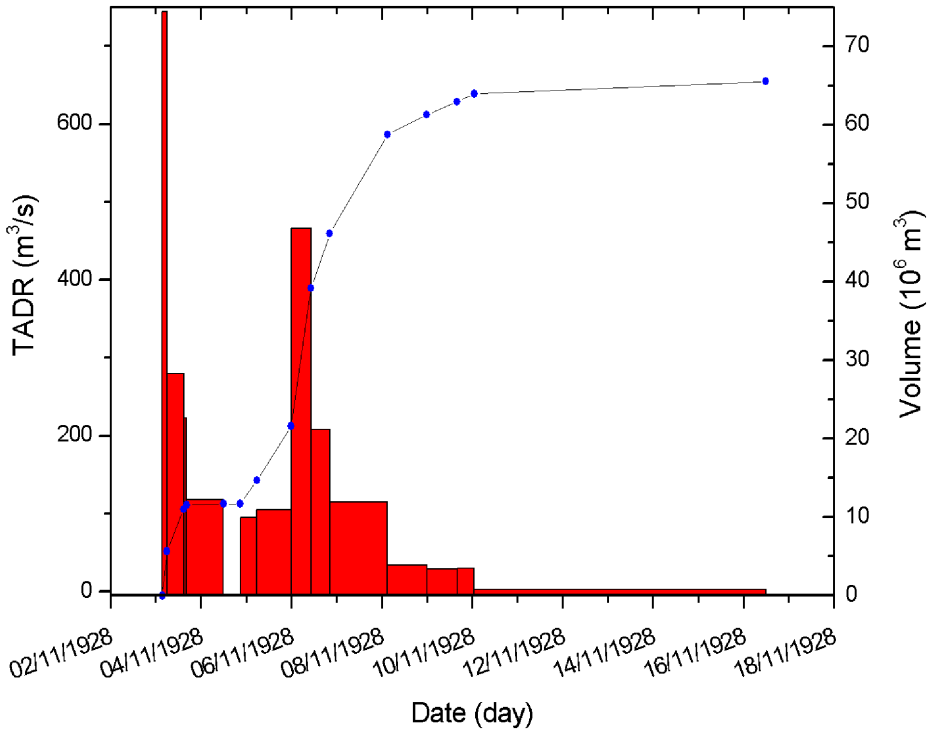

Figure 2.13: Time averaged discharge rates (TADR), on the left axis, and cumulative volumes, on the right axis, of the 1928 eruption

Chapter 3

A model for the eruptive mechanism of the 1981 eruption

The TADR trends of basaltic eruptions can be divided by the maximum value into two part, the waxing and the waning phases ([34]). In the waxing phase, often characterized by a short duration, the TADR rapidly reaches its maximum values, then in the longer waning phase the TADR shows an exponential decreasing to low values until the eruption end. This mechanism is common to the TADR trends of the 2001, 1981 and 1928 Etna eruptions. On the contrary a large difference in the magnitude of the peak values of the 1981 and 1928 eruptions against the 2001 is evidenced.
Given the peculiarity of the 1981 eruption, we choose to analyse its TADR trend for studying a possible eruptive mechanism. Also the 1928 eruption showed an extraordinary peak discharge rate that deserves further investigations.

3.1 Analysis of the 1981 Etna eruption TADR trend

Several authors have previously estimated the total volume, the averaged effusion rate and the eruption rate of the 1981 Etna eruption. Romano and Vaccaro ([62]) reported a total volume of $30 \cdot 10^6 m^3$ and the eruption rate of 58 m^3/s.

Guest et al. ([37]), who studied the flow-field development of the 1981 eruption, reported a total volume of $20 \cdot 10^6 m^3$ and an average effusion rate of 128 m^3/s in the first 40 hours. Del Negro et al. ([35]) roughly estimated the average effusion rate during the first 24 h reporting that it might have approached 300 m^3/s, a large value for Etna eruptions.
Through the analysis of the TADR trend it was possible to estimate a maximum value of 640 m^3/s that was reached in a very short time which is quite unusual for known Etna eruptions. If we consider for comparison the 2001 eruption ([20]) (fig. 3.1), it is clear that, even though the shape of the TADR trend of its main flow resembles very well that of the 1981 eruption, the maximum values are very different, reaching 32 m^3/s and 640 m^3/s, respectively. The high TADR values

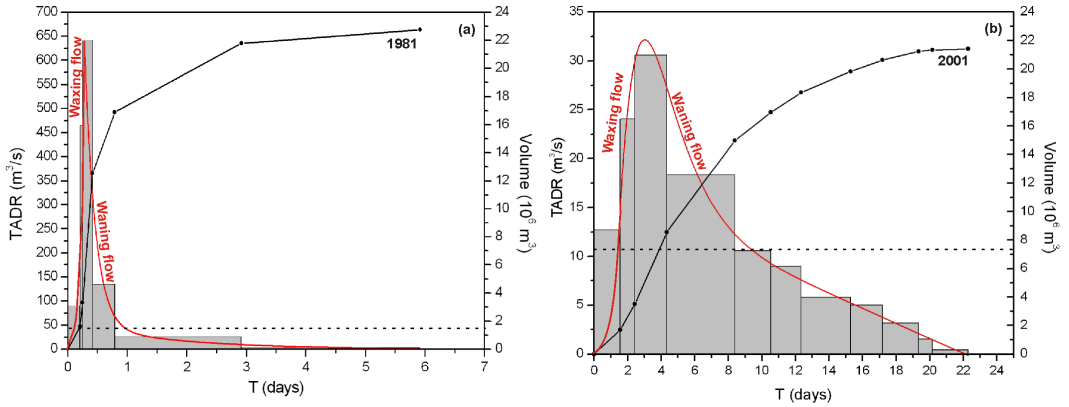

Figure 3.1: TADR on the left axis, and cumulative volumes, on the right axis, of the 1981 eruption (a) and of the main lava flow of the 2001 eruption (b). Red lines shows the interpolated discharge rate trends (using an exponential fit and a log function for the 1981 and 2001 eruptions, respectively) that illustrate the waxing and waning phases for both lava flows. The range of the left axes (TADR) of (a) is 20 times that of (b), the range of the (a) and (b) right axis (volume) are the same, the range of the x axes (T) of (a) is shorter than that of (b): 7 versus 25 days

observed for the 1981 eruption requires an explanation that was conceived after a comparative analysis among a number of basaltic eruptions from Etna and other volcanoes, for which effusion and eruption rate values are available in literature. The eruption rate is available for 60 Etna flank eruptions occurring between 1607 and 2008 ([10] ; [12] ; [13]; [61] ; [68] ; [75]). These values are plotted against the corresponding durations and volumes (Fig.3.2) and show that the 1981 erup-

tion, with a value of 44.5 m^3/s, is located at the high end of the Etna eruption plot. However, the eruption rate cannot be considered as a significant parame-

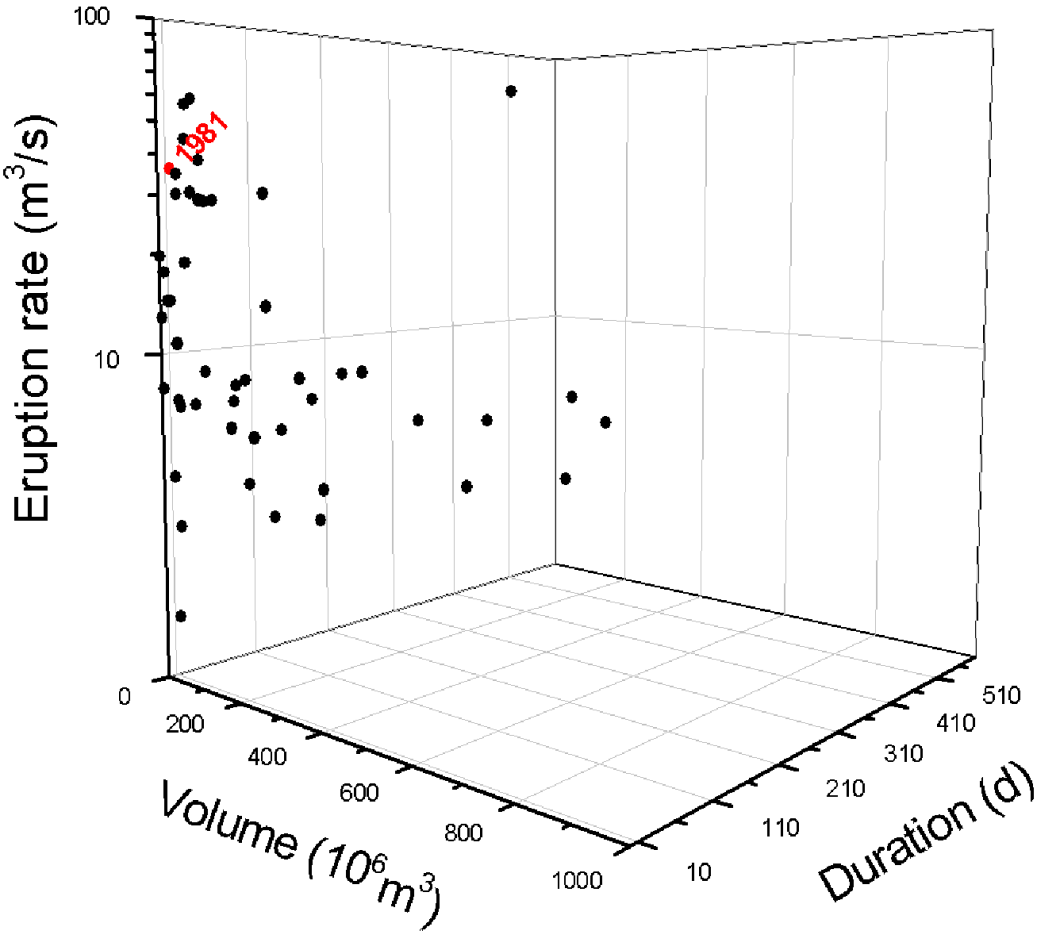

Figure 3.2: Comparison between the duration and the, here evaluated, eruption rate and volume of the 1981 eruption with the values reported in literature for 60 Etna flank eruptions occurred between 1607 and 2008 ([19]).

ter for assessing the intensity of an eruption because it does not highlight events characterized by high rates and short durations. A second comparison has been made by considering a reduced dataset including only those events for which the maximum effusion rate was known (Tab.3.1;Fig.3.3). As shown in figure 3.3, the 1981 eruption was very different from other Etna flank eruptions whose max rate is always below 100 m^3/s . In the same plot a set of well-documented basaltic eruptions from other volcanoes (Kilauea, Mauna Loa, Nyiragongo and Piton de

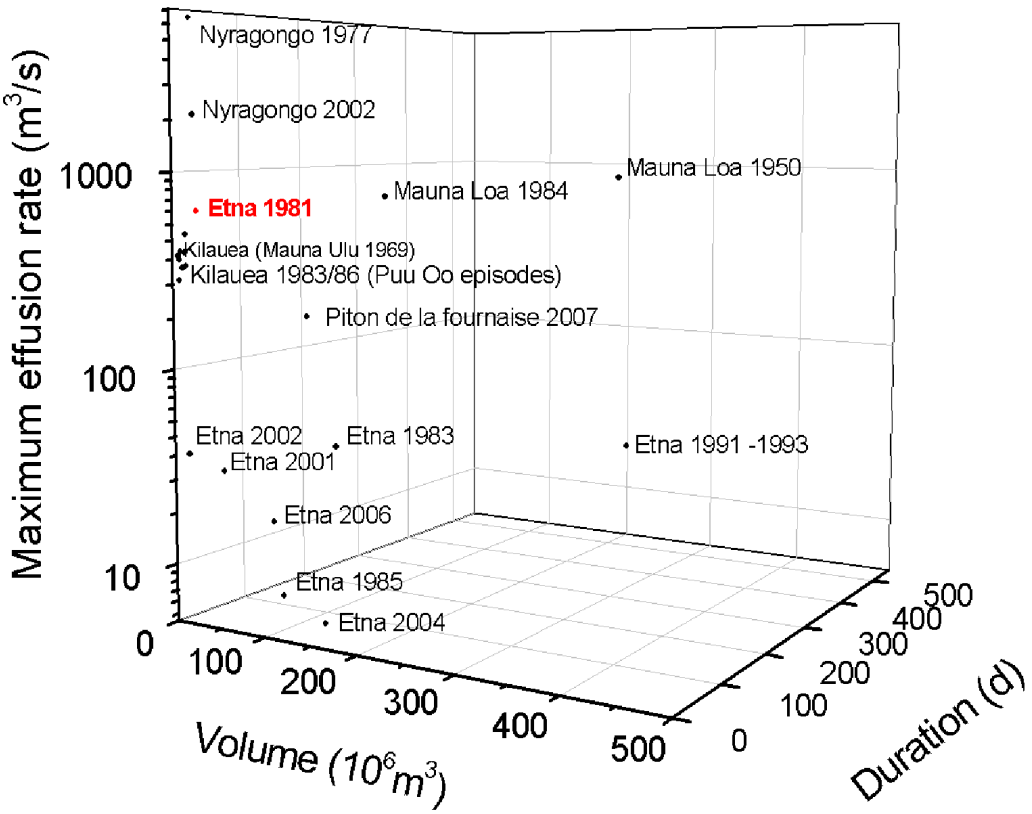

Figure 3.3: Comparison between the duration and the, here evaluated, maximum effusion rate and volume of the 1981 eruption with the values reported in literature for post-1971 eruptions of Etna (Tab.3.1) and selected eruptions from other volcanoes (Tab.3.2)

Etna eruption	**Volume** ($10^6 m^3$)	**Duration** (days)	**Max. effusion rate** (m^3/s)	**Data source**
2006	42.14	94	15.00	[77]
2004	40.00	182	3.00	[53]
2002 N fissure	9.80	9	55.00	[44]
2001	40.10	23	30.68	[20]
1991 - 1993	235	473	22.00	[14]
1985	30	125	5.00	[39]
1983	90.00	131	35.00	[39]
1981	22.75	6	640	this work

Table 3.1: Volume, duration and maximum effusion rate for Etna eruptions.

la Fournaise) showing high effusion rates (Tab.3.2; Fig.3.3) are included. Since the 1981 eruption appears close to these eruptions than to those of Etna, their eruptive mechanisms are discussed below with the aim of finding similarity with the 1981 eruption ([19]).

3.2 Description of eruptions with high effusion rate

Kilauea and Mauna Loa eruptions showed high effusion rates which were associated with strong lava fountaining ([63]). On Kilauea, the Mauna Ulu lava fountains were typically hundreds of meters high up to 540 m ([63]) while those produced during four short Puu Oo episodes in 1984 and in 1985 were between 352 and 441 m high ([41]). On Mauna Loa, huge effusion rates were related to the development of very long curtains of fire associated with broad lava fountaining tens of meters high ([63]). The Nyiragongo eruptions of 1977 and 2002 exhibited very fast advancing lava flows resulting from the emptying of a lava lake located in the large summit crater of the volcano. In the 1977 eruption an extremely fluid, fast-moving (up to 60 km/h) lava flow drained the summit lava lake and covered several villages in a very short time ([76]). During the 2002 eruption, several fissures opened on the S and NW flanks of the volcano, the upper fissures drained

Other volcanoes	**Date**	**Volume** $10^6 m^3$	**Duration** (days)	**Max. effusion rate** (m^3/s)	**Data source**
Kilauea (Mauna Ulu, phase 11)	1969	8.9	0.3	342	[73]
Kilauea (Puu Oo, episode 26)	2 nov. 1984	6.6	0.2	382	[41]
Kilauea (Puu Oo, episode 36)	2 set. 1985	11.5	0.4	333	[41]
Kilauea (Puu Oo, episode 37)	24 set. 1985	14.7	0.5	340	[41]
Kilauea (Puu Oo, episode 39)	13 nov. 1985	13.7	0.4	396	[41]
Mauna Loa	1950	440	23	1044	[63]
Mauna Loa	1984	220	20	806	[48]
Nyiragongo	1977	21	2	5833	[76]
Nyiragongo	2002	14	2	1944	[28]
Piton de la Fournaise	2007	130	29	200	[72]

Table 3.2: Volume, duration and maximum effusion rate for other volcanoes

the summit lava lake whereas the lower fissures were supplied from a dike rising directly from the shallow plumbing system, forming lava flows that destroyed part of the city of Goma ([5]). The maximum effusion rates (Tab.3.2) for the 1977 and upper fissures of 2002 eruptions can be estimated by the lava volumes reported in literature (21 $10^6 m^3$; [76] and 14 $10^6 m^3$; [28], respectively) even if the duration of the lava effusion is more uncertain due to scarce available information. Tazieff [1977] reports less than 1 hour for the 1977 eruption, whereas the upper fissures of the 2002 eruption were active for at least 2 hours ([5]). These combined volumes and durations provide maximum effusion rates of about 5833 and 1944 m^3/s for the 1977 and 2002 eruptions, respectively. As these values are amongst the highest ever observed for a lava flow and because of uncertainties in volume and duration, they can only be considered a rough estimate. An huge effusion rate was also observed during the April 2007 eruption of Piton de la Fournaise, when the Dolomieu crater at the summit collapsed ([21]). This eruption started with a dike propagating from the shallow plumbing system below the Dolomieu crater toward the lower flank where lava flows were discharged at about 65 m^3/s. The fast magma outpouring caused a sudden decrease in pressure inside the shallow reservoir that induced the collapse of the summit roof. The rock column collapsed into the reservoir and acted as a piston, increasing its internal pressure and causing the rapid drainage ([54]). The maximum effusion rate during this paroxysmal phase has been estimated to be more then 200 m^3/s ([72]) which is quite a large value for the effusive eruption of this volcano that generally shows low effusion rates (from $< 2m^3/s$) for summit eruptions and up to about 20 m^3/s for the initial phases of flank eruptions ([21]). During the 1981 Etna eruption lava fountaining from F1 fissure, 100-200 m high ([45]), formed short-lived lava flows that accounted for only 3% of the total volume and had an average discharge rate of 90 m^3/s. The main fissure, F2, presented only minor explosive activity. A curtain of lava, indicated by the large spatter rampart along this fissure, was formed by low (few meters to about ten meters high) lava fountains, as proved by the lack of pyroclastic deposits that conversely are present on the eastern side of F1,a,b,d fissure, while the most voluminous lava flow occurred (87% of the total volume associated with the maximum discharge rate of 640 m^3/s). Finally, F3 fissure produced mild strombolian activity and a minor lava flow (6% of the total volume at an average discharge rate of 3 m^3/s). Therefore the magnitude of the maximum discharge rate of the 1981

Etna eruption cannot be associated with an eruptive mechanism similar to those of the Kilauea and Mauna Loa eruptions, which are characterized by strong lava fountains of gas-rich basaltic magma that generate lava flows. On the contrary, a mechanism similar to that of Nyiragongo and Piton de la Fournaise eruptions, where the extraordinary effusion rates are clearly associated with sudden pressure changes in shallow plumbing systems or superficial reservoirs, can be inferred to explain the evolution of the 1981 eruption.

3.3 Discussion on the eruptive mechanism

The results obtained in this work and the analysis presented in previous paragraph provide useful insights for investigating its eruptive mechanism. A variety of hypotheses for the mechanism of this eruption have been proposed in literature. Sanderson et al. [1983] modelled the dike feeding the eruption using precise levelling and gravity data showing that, between August and September 1980, the magma rose from depth, filling a SSE-NNW trending fissure zone. In March 1981 a long eruptive fissure opened on the NNW flank due to a deeper radial intrusion of magma, as testified by the gravity change measured. Scott ([67]), on geochemical and petrographic basis, suggested that the 1981 eruption radially drained a hybrid magma that was the result of mixing residual 1979 magma with fresh magma during the dike filling from September 1980. Bonaccorso ([11]) re-analysed the levelling data set of Sanderson et al. ([64]) and compared it with EDM data acquired between October 1979 and May 1982. He proposed a double-source model consisting of two tensile dislocations; the first associated with deeper magma injected at depth and the second related to magma ascent in the summit area that activated the eruptive fissure. Carbone et al. ([15] applied a parametric inversion analysis of previous data (microgravity, levelling and EDM) and showed that when a two-tensile crack model is used ([11]) the observed vertical and horizontal ground deformations are underestimated. Therefore they suggested that the ascending magma filled a network of pre-existing interconnected fractures, allowing mass redistribution with no evident deformation. They also suggested that the significant effusion rates could be related to a low viscosity magma. The previously described models do not take into account the cause of both the peculiarly rapid evolution of the eruption and the exceptional value of its maximum discharge

rate, except for the hint on low viscosity magma given by Carbone et al. ([15]). Indeed they envisaged a complex intrusive mechanism that drove the eruption, suggesting that up to two magma sources may have fed the eruption. As already outlined, the TADR trend resembles the general shape of a typical Etna eruption, except for the maximum value (640 m^3/s). Such a value cannot be linked to the typical processes involved in some strong basaltic lava flow eruptions, i.e. vigorous magma injection of a gas-rich basaltic magma into an over pressurized dike ([63]) or low viscosity magma. The former mechanism should be excluded because high lava fountaining was not observed during the main phase of the eruption. The latter mechanism is unlikely because the chemical composition of the 1981 lava is a hawaiite ([67]) similarly to other Etna eruptions ([62]) that did not have high discharge rate.

3.4 The 1981 eruptive mechanism model

We suggest that, the magnitude of the maximum discharge rate can be ascribed to rapid drainage of a shallow or superficial reservoir and we identify four different phases below described to explain the phenomena observed during the 1981 eruption.

Phase 1. A long pre-eruptive phase was characterized by the ascent of magma inside the shallow plumbing system, as indicated by the strombolian activity and periodic ash emissions observed at the summit craters since the spring of 1980. In particular, three paroxysmal explosive episodes occurred from the NEC on 1st and 6th September 1980 and 5th February 1981 ([64]). These explosive events were accompanied by abundant overflows of lava that represent a clear evidence of new magma rising from depth. We suggest that this magma filled the shallow part of the plumbing system, building a small magma reservoir inside the volcanic pile. The complete filling this reservoir caused the uprush of magma and a series of short-lived summit lava flow eruptions.

Phase 2. The 1981 eruption started with the opening of fissures F1a, F1b, F1c and F1d, at progressively lower altitude, accompanied by lava fountains about 200 m high [SEAN, 1981], as evidenced by tephra deposits dispersed to the west of F1a, F1b and F1d. Short-lived lava flows were also emitted. The volume of these lava flows and of the pyroclastic deposits is estimated to be 1.62 $10^6 m^3$ (only 7% of the

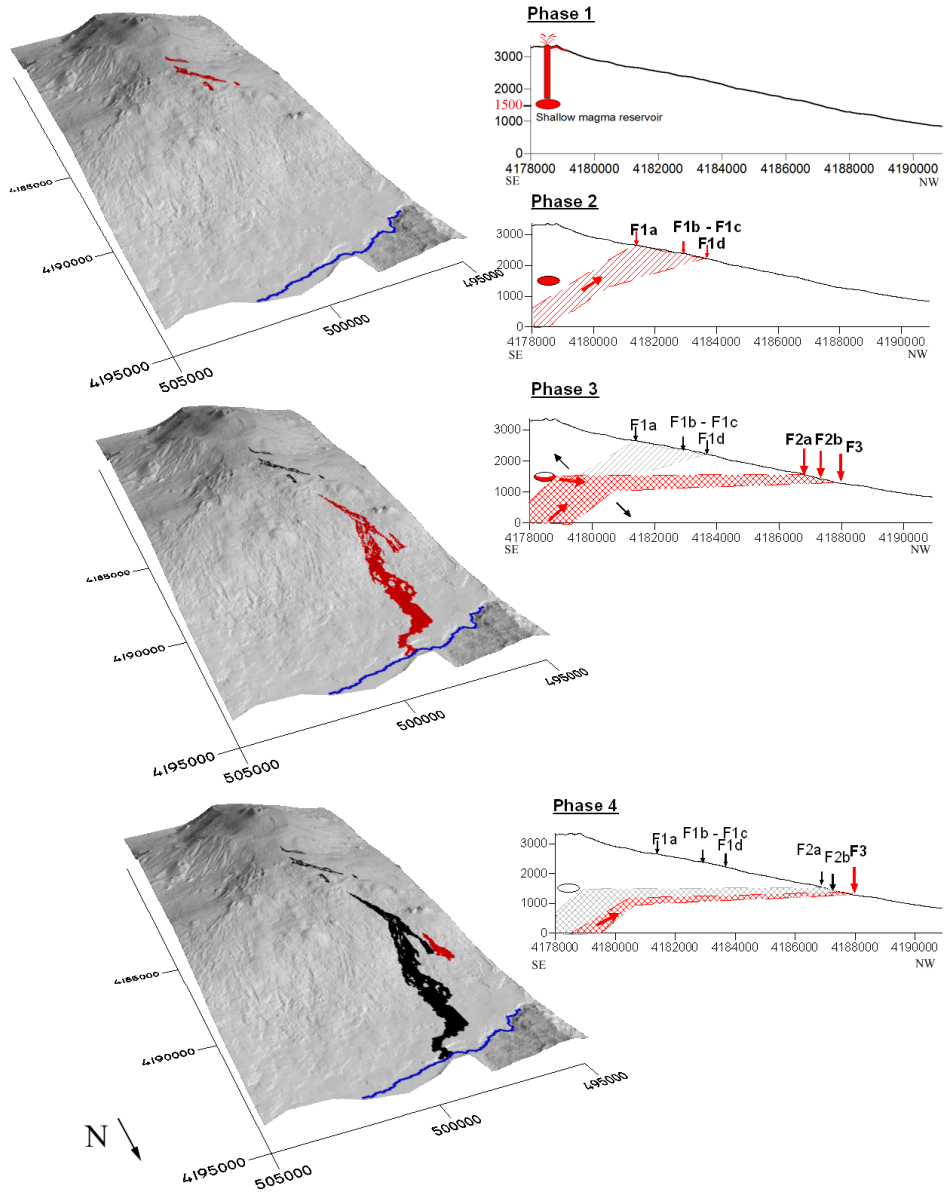

Figure 3.4: Eruptive mechanism proposed in this work to explain the observed TADR. The dike feeding the eruptive fissures, identified by the dashed lines, is sketched but it is not dimensioned. The perspective views on the left show, during each phase, the active lava flows (red) and not active (black). The X and Y axis, in the perspective views, show the East and North coordinates expressed in the UTM-WGS84 system while in the right figures the X axes show the North coordinates and the Y axis show the height above sea level ([19]).

total volume) corresponding to a TADR of about 90 m^3/s. The opening of these fissures can be related to a dike intrusion from the deeper part of the plumbing system located around 3 km below the sea level ([16]) and the consequent arrival of a gas-rich magma that was responsible for the explosive activity. To estimate the magma driving pressure (Γ) at the F1 fractures we used the cubic law ([65]) i.e. the equation used to calculate fluid flow rate (Q) between two parallel plates:

$$Q = \frac{\Gamma \cdot w^3 \cdot L}{12 \cdot \eta} \tag{3.1}$$

where L and w are fissure length and opening, respectively and η is the viscosity. We consider the estimated TADR of $F1 = 90\ m^3/s$, $\eta = 135 Pa \cdot s$ (evaluated as below described), a fissure width $w1 \simeq 1m$ ([11]; [65]) and a length $L1 = 734\ m$ which is the sum of the $F1a, b, d$ lengths. These fissures represents the intersection with the surface of the deep-seated dike because they erupted as lava fountaining, while the F1c was not considered because it has a different orientation and emitted only lava flow, therefore it represents a local and very shallow propagation of the F1b fissure. The lava viscosity $\eta = 135\ Pa \cdot s$ was evaluated by considering the viscosity law of a hydrous Etna basalt ([36]), a water content of $0.3 wt.\%$ ([67]) and an temperature T=1100 $°C$, which represents a plausible value of pre-eruption temperature of a magma flowing into the dike since most of measured eruptive temperature of Etna lava flows range between 1080 - 1095 $°C$ ([58]). Using these values, and the cubic law equation, we evaluate a driving pressure $\Gamma 1 \simeq 0.15$ MPa/km, necessary for generating the observed TADR of 90 m^3/s.

Phase 3. The main phase of the eruption began with the opening of F2 fissure, from which a large lava flow was emitted. A Spatter-rampart forming explosive activity was also observed, however the explosivity index (E), which is the percentage of the total volume that is pyroclastic material, is low ($E = 2.8$) during this phase with respect to Phase 2 ($E = 33.3$). This observation suggests that F2a was, at least partially, fed by a gas-depleted magma that had resided for a certain period in an open reservoir into the shallow portion of the plumbing system. This is in agreement with petrological analyses ([67]). Therefore we suggest that during Phase 3 the previously intruded dike (Phase 2) have expanded the surrounding wall rocks, intercepting and draining the shallow magma reservoir previously re-filled (Phase 1). The cubic law equation was used to estimate the

driving pressure $\Gamma 2 \simeq 0.44 MPa/km$ necessary for generating from the F2a fissure a discharge rate as high as 640 m^3/s, considering a length $L2 \simeq 1760m$ and width $w2 \simeq 1m$ ([11]; [65]). Since $\Gamma 1$ is lower than $\Gamma 2$ the dike intrusion from the deeper part of the plumbing system alone was not sufficient for explaining the F2 maximum discharge rate. The discrepancy between the two values of the driving pressures can be seen as the key factor to explain the eruptive mechanism of the 1981 Etna eruption. An overpressure in the magma reservoir of about 4.41 MPa was determined using the relationship described in Wadge ([79]):

$$P = \rho m \cdot h \cdot g - \rho v \cdot h \cdot g \tag{3.2}$$

where ρm (magma density) = 2650 kg/m^3, ρv (volcanic pile density) = 2400 kg/m^3 ([79]) and h is the depth of the magma reservoir that we hypothesized to be at 1800 m below the summit, in consideration of the elevation of the main vent. This overpressure produces, over a distance of about 9 km, measured between the reservoir and F2, a driving pressure of 0.49 MPa/km. By inserting this value in the cubic law and the dimension of F2 a discharge rate of 710 m^3/s that has the same order of magnitude of the measured value. The inflow of magma from the reservoir into the dike led to a sudden pressure rising which triggered a horizontal propagation of the dike. This resulted in the opening of a shallow NNW crack along which the F2a and then F2b fissures emerged at lower elevation than F1. Such a rising pressure in the shallow dike caused the high discharge rate of 640 m^3/s from F2. Thus the significant volume of erupted lava and of the spatter rampart (19.83 $10^6 m^3$), which account for the 87% of the total volume, can be associated to the described draining process.

Phase 4. The dike continued to propagate and the opening of another fissure (F3) produced a rapid pressure fall in the plumbing system. This caused, for a feedback mechanism, the collapse of the summit craters as evidenced by continuous and strong ash emission observed during the eruption ([78]; [45]). During this final phase (from 20th March to the end of the eruption) the F3 fissure produced effusive and low explosive activities. Lava flowing towards the village of Randazzo progressively slowed and stopped after 3 days. The low volume of this lava flow and the very low TADR (3 m^3/s) suggest that F3 vent was fed during the waxing phase of the dike and was no longer supplied by the shallow magma reservoir. In

fact, a weak explosive activity (hornito-forming spatter ejection) occurred at the lower vent evidencing that the dike emptying was driven only by residual magma degassing.

3.5 Conclusive remarks

The analyses of the temporal evolution of the 1981 Etna eruption showed that the 1981 eruption is dissimilar from the others because it had a very high value (640 m^3/s) which has never been recorded in recent Etna activity. The analysis was extended to other volcanoes presenting comparable high values, i.e. Kilauea, Mauna Loa, Nyiragongo and Piton de la Fournaise. The eruptive mechanisms of these volcanoes are different from those usually associated with Etna flank eruptions and thus provided useful insights for the interpretation of the behaviour of the 1981 eruption. More specifically, the analysis of some recent eruptions of these volcanoes suggested that the rapid evolution of the 1981 main flow and its huge discharge rate can be related to a sudden emptying of a shallow magma reservoir interacting with a dike intrusion from the deeper part of the plumbing system. The complex interaction between an eruption feeder dike and a small shallow reservoir, that often built up within basaltic volcanic edifices, proposed for the 1981 eruption can be applied to understand similar lava flow eruptions which produce fast moving and dangerous lava flows. Finally, the reconstruction here presented, improves the knowledge of the 1981 eruption characterized by very fast moving lava flows, which are uncommon within Etna eruptions despite they represent a serious concern for the safety of potentially inundated areas. Future hazard evaluations should take into account that an eruption characterized by a rapid evolution can be foreseen if, thanks to improvements in monitoring systems, signs of the formation of shallow magma reservoirs inside the volcanic edifice are detected.

Chapter 4

Analysis and design of diversion barrier

In order to mitigate the destructive effects of lava flows along volcanic slopes, the building of artificial barriers is a fundamental action for controlling and slowing down the lava flow advance, as experienced during a few recent eruptions of Etna: in 1983, 1991-1993, 2001 and in 2002, when earthen barriers were built to control lava flow expansion with different level of success. In this chapter, starting from the study of mitigation actions against lava flow invasion adopted at Etna, an engineering approach to design the lava barriers is proposed. The design of a gabion structure is presented in comparison to the classical earthen barrier. Finally, an experimental test performed to evaluate the assembling and transportation procedure after gabions filling was illustrated.

4.1 Case history of mitigation actions against lava flow invasion at Etna

The concept of slowing and diverting lava flows by means of artificial barriers for guiding their paths arose from the observation of lava encountering natural morphological obstacles or pre-existing barriers. These cases were experienced

when the lava flow approached Catania's city walls in 1669. Barrier construction represents the first step that can be undertaken in order to delay the lava advance, especially as regards to the most dangerous eruptions, such as those originating from low altitude vents and in proximity of inhabited areas ([50]). These activities should be combined with other types of mitigation actions, including population evacuation. In the 1983, the intervention against lava flow invasion was aimed to deviate the flow path in an artificial channel, excavated parallel to the natural one. Earthen barrier were built to guide the path of the diverted lava by blocking lateral expansion in built-up or farmed areas. Explosives were utilized to create an opening in the solid levee of the lava channel at the junction with the artificial one. A number of difficulties prevented the placing of charges in the deepest part of the lava levee, thus a modest diversion was created and it was supplied only a couple of days ([4]). As a matter of fact the little slope of the artificial channel and the exposition of fresh lava to the atmosphere facilitated the lava cooling and consequently the artificial channel was obstructed soon. However, the dumping of a large amount of big solid fragments produced by the explosion into the lava channel plugged the tunnel located just downhill from the point of intervention, forcing nearly all the lava to overflow out of the tunnel ([8]). This intervention was a partial success but demonstrated that man can effectively control the development of a lava flow. During the 1991-1993 eruption ([14]) the lava flow approached Zafferana, 8 km away from the vent, and, through a simple computer simulation, the identified lava flow path showed that the town was likely to be inundated ([26]). The measures to protect Zafferana included the building of four lava containment earth barriers and several attempts at plugging the lava tube by throwing concrete blocks, steel hedgehogs and large fragments of solid lava into a skylight close to the vent. Downhill, the earth barriers, oriented orthogonally to the direction of the lava flow, slowed the front propagation down for a few weeks although they were not able to stop it altogether. Lava overflowed on the earth barriers, thus inducing the Civil Protection authorities to carry out a drastic lava flow diversion near the vent. Finally, the lava flow was totally diverted into an artificial channel by blasting the wall separating it from the natural channel and obstructing downstream the natural tunnel ([8]). During the 2001 eruption, lava flows emitted by seven vents propagated mainly on the southern flanks of Etna ([20]). The lava flows emitted from the 2700 and 2550 m a.s.l. vents threatened the

tourist facilities on the Rifugio Sapienza area. Thirteen earth barriers were built up to protect the area, initially delaying the advance of the flows and then diverting it toward SE, away from the aforementioned facilities. The first five upper barriers were almost totally buried by the lava flowing down the slope, whereas the four barriers erected close to Rifugio Sapienza for diverting the approaching flow were successful partially thanks to the decreasing effusion rate ([7]). The 2002-2003 eruption produced two lava flows which covered both the north eastern and the southern Etna flanks. On the north eastern side a flow, active between 26 October and 7 November 2002, partially covered the tourist facilities of Piano Provenzana. On the South flank the effusion lasted until 28 January 2003 threatening once again the Rifugio Sapienza area. A great effort was devoted to the construction of earthen barriers: six barriers (five on the south and one on the north-east flank), oriented about 30 degree with respect to the main direction of the flow, were erected to contain the flow in correspondence of the touristic facilities (Personal Communication, Italian Department of Civil Protection). These actions, taken in accordance with the local authorities including the "Park of Etna", contributed to mitigate the effect of the lava flows advance considering that on the 24 November the lava flows directed toward south was deviated away from the touristic facilities of "Rifugio Sapienza". Unfortunately, on 16 December the lava overflowed from the barrier destroying two buildings and cutting the "SP92" road before stopping soon after.

4.2 Design of a gabion structure

The analysis of Colombrita ([18]) about the earth barrier built during 1983 Etna eruption shows that the main problem of this kind of intervention is the great amount of material to be moved, the distance between the quarry and the site, the access road. In this work a different type of engineering work was analysed that could be adopted for the construction of a lava-containing barrier, which would improve the efficiency of the structure: the gabions (fig. 4.1). In civil engineering a gabion wall is a retaining wall made of rectangular containers (baskets) fabricated of thick galvanized wire, which are filled with stone and stacked on one another. The most common civil engineering use of gabions is to stabilize shorelines or slopes against erosion. Other uses include retaining walls, temporary flood walls,

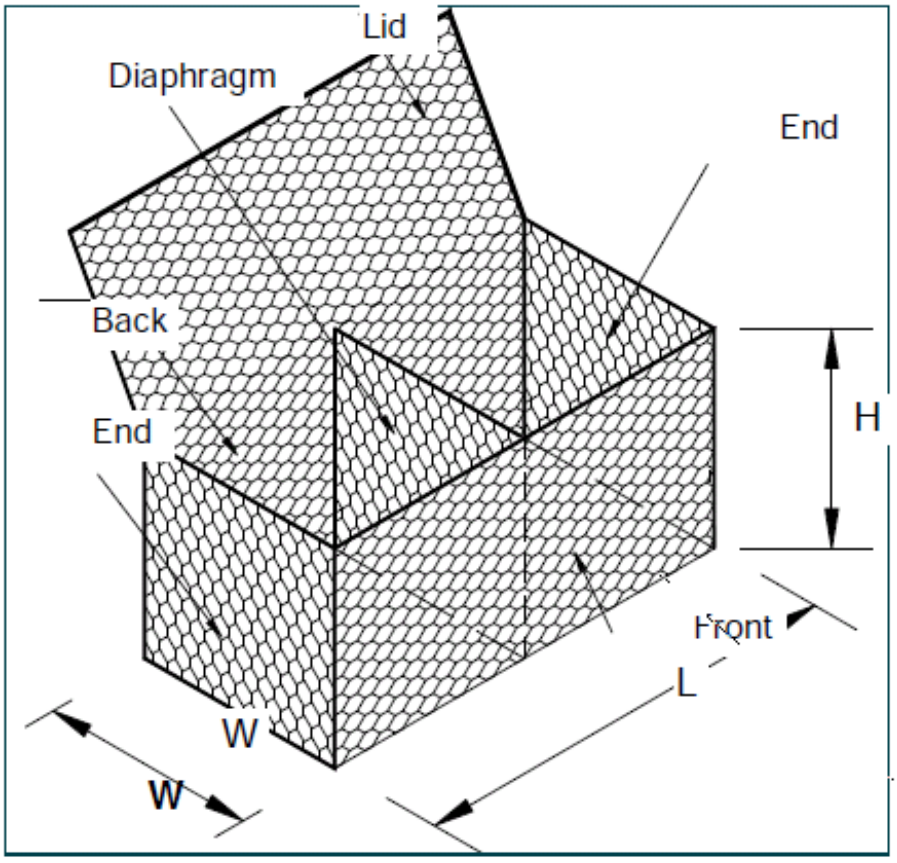

Figure 4.1: An example of gabions structure by Maccaferri S.p.a.

to filter silt from run-off, for small or temporary/permanent dams, river training, channel lining. They may be used to direct the force of a flow of flood water around a vulnerable structure. Gabions have some advantages over loose rip-rap because of their modularity and ability to be stacked in various shapes; they are also resistant to being washed away by moving water. Gabions also have advantages over more rigid structures because they can conform to ground movement, dissipate energy from flowing water, and drain freely. In this study we have proposed to use the gabions to construct a lava barrier. They appear specifically appropriate for building a lava flow barrier, particularly if they can be filled with blocks of lava located in proximity of the area of interested.

4.2.1 Evaluation of the stability of a gabion barrier

In order to evaluate the stability of a gravity wall it is necessary to verify the stability against sliding and overturning, as well as the load-bearing capacity of the foundation soil. In this study, only the stabilization of a gravity wall from sliding is taken into account, thus giving:

$$S = \frac{R}{T} \tag{4.1}$$

where S is a safety coefficient, R is the stabilization force (P and F) and T is the destabilization force (L) (fig. 4.2) (for L see section 4.3. On the basis of the

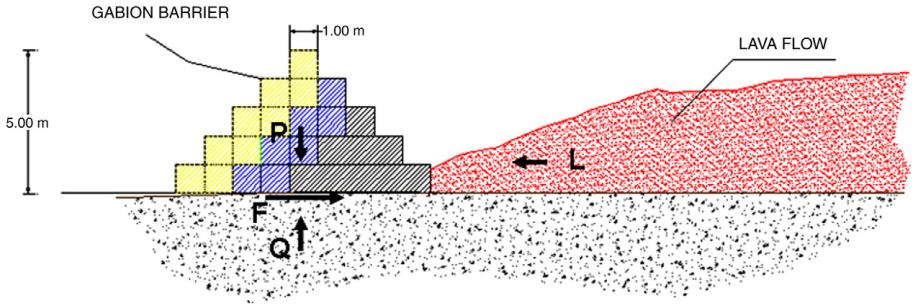

Figure 4.2: Configuration of a gabion barrier: wall height can be increased by adding and interlocking new elements.

stabilization requirement for gabions S must be greater than 1.3 (D.M.11.03.88). To calculate L we assumed that the liquid lava density was 2.7 g/cm^3, the gravity

Characteristics of the wall	
Height	From 3 to 10 m
Gabion porosity	30%
Rock fill unit weight	20 KN/m^3
Materials acting on the barrier	
Lava unit weight	27 KN/m^3
Average slope	20°
Foundation	
Soil unit weight	27 KN/m^3
Friction angle and slope	20°

Table 4.1: Input data for planning a gabion barrier.

acceleration was 9.8 m/s^2 and the terrain slope (β) was equal to 20°. L was calculated for barriers with a height between 1 and 10 m, the width of the lava front was set to 1 m and the length of the lava front was assumed to be equal to its height ([47]). In order to evaluate the stability of a gravity wall we used GawacWin software ([1]) which was developed to provide engineers with a tool to conduct stability analyses on gabion retaining walls. The program uses the limit equilibrium (optimized through the Simplex Minimize Algorithm) to check the overall stability of the structure. The software takes into account the mechanical characteristics of gabions manufactured by Maccaferri Group and it is able to determine the safety coefficient against wall sliding, overturning, bearing capacity failure (evaluating the normal pressures acting on the terrain below the base of the gabion wall), and failure along each gabion layer interface. In addition, a global safety coefficient (S) may be determined along any surface surrounding the wall. The program's main calculation hypothesis is to consider the problem as having a planar configuration, requiring only the cross-section dimensions for the analysis. In such a hypothesis the effects caused by variations in the loads or in the soil geometry in a perpendicular direction to the plane can be neglected. The input data (tab. 4.3) are relative to the characteristics of the wall (batter, width, height, gabion porosity and rock fill unit weight) and those of the materials acting on the barrier (unit weight and average slope of the foundation, soil unit weight, cohesion, friction angle and slope). The output report provides the position of the surface of application of the active thrust and the value, direction and

point of application of both the active thrust and the available passive thrust. Additionally, it computes the proper weight structure and the applied loads, the reaction forces (normal and tangential under the base) and finally, the available resistance along the base. In this work we used an iterative process by changing the data input so as to obtain the equivalence between the calculated force and the active thrust that resulted from the GawacWin computation. The processes terminated when a safety coefficient S greater than the threshold of 1.3 established for this type of structure was obtained. The number of gabions necessary for the construction of the barriers could be estimated once its geometrical dimension has been established. The size of gabions are 2 m long, 1 m wide and 1 m high to allow more easy transport and positioning in an emergency situation. Finally, a sensitivity analysis on the software adopted for dimensioning the gabion barriers was performed to understand how the stability of the barrier is influenced by the gabion porosity and by the unit weight of the filling material. The results showed that a barrier 4 m high filled with lava block for which we have considered a unit weight of 20 KN/m^3 is still stable ($S > 1.35$) with porosity values up to 50%. Whereas if we considered a less dense material (unit weight as low as 14 kN/m^3) the porosity value should be lower than 30%. Thus the structure is stable for ranges of porosity and unit weight wider than those valid for the material available on site demonstrating that the barrier can be built with heterogeneous blocks without requiring any preliminary handling ([66]).

4.3 Estimation of lava pressure on the barrier

To estimate the lava pressure (L) on the barrier we initially adopted a simplified approach, assuming that the lava is a Newtonian fluid, an assumption that can be made when the temperature is high and the crust can be assumed to be thinner than the core ([46]). Thus, the lava pressure on the barrier can be expressed as:

$$L = \rho \cdot g \cdot h \cdot l \cdot w \cdot \cos\beta \tag{4.2}$$

where ρ is the density, g is the gravity acceleration, h, l and w are the height, length and width of the lava front, respectively, and β is the terrain slope. This simplified approach did not take into consideration the lava cooling, and subse-

quently the non-newtonian rheology. The non-newtonian rheology causes a remarkably lower flow rate compared to a Newtonian flow of the same viscosity ([74]). Consequently, the considered lava pressure force that affects the barrier is overestimated and so the wall could result over-dimensioned. Therefore, to better quantify the lava pressure on the barrier, a finite element model was implemented considering the lava as a fluid in transient analysis to study the effect of temperature. In fact, the lava behaves as a Newtonian fluid when it is close to liquidus temperature while, at lower temperatures, it behaves as a pseudoplastic fluid. As a consequence a particular a power - law rheology can be adopted for basaltic lavas ([38];[71];[55];[69]). The power - law rheological parameters are temperature - dependent and this has a great effect on the behaviour of lava flows (e.g. [56]; [57]; [31]).

In the following we consider a horizontally layer of lava in contact with a barrier and a power-law rheology with temperature dependent rheological parameters as in [57] and [56]. The model adopts the Navier Stokes equation for incompressible flow in bi-dimensional configuration (eq. 4.3), the continuity equation (eq. 4.4) and the heat transfer equation (eq. 4.5).

$$\rho \cdot \frac{\delta u}{\delta t} + \rho(u \cdot \nabla)u = \cdot \left[-pI + \eta(\nabla u + (\nabla u)^T\right] + F \tag{4.3}$$

$$\nabla \cdot u = 0 \tag{4.4}$$

where ρ is the density, u is the velocity, p is the pressure, η is the viscosity and F represents the gravity force.

$$\rho C_p \frac{\delta T}{\delta t} + \nabla \cdot (-k\nabla T) = Q + q_s T \tag{4.5}$$

where T is the temperature, ρ is the density, C_p is the specific heat capacity at constant pressure, k is the thermal conductivity, Q is the heat source, q_s is production - absorption coefficient.

As to the constitutive equation, we assume the power law:

$$\sigma_{xz} = 2K\dot{e}_{kz}^n \tag{4.6}$$

where σ_{xz} is the viscous stress, $\dot{e}_{kz}$ is the strain rate, K is the consistency and $0 <$

Parameter	Value
ρ	2700 kg/m^3
v_in	0.2 m/s
T_L	1400 K
c_p	837 $J/(kgK)$
a	$2.7 \cdot 10^-4$ K^-2
n_0	1
K_0	10^-27Pa $\cdot s$
b	$10^5 K$

Table 4.2: A choice for the value of parameters.

$n \leq 1$ is the power low coefficient. We introduce a dependence of the rheological parameters n and K on temperature. For n we adopt the function of temperature in Piombo and Dragoni ([57]) that fits the measurements of Pinkerton and Norton ([55]), which refer to basaltic lava of Mt. Etna a temperature range between 1360-1393 $°K$

$$n(T) = n_0 - a(T - T_L)^2 \tag{4.7}$$

where n_0 and a are constants, and T_L is the liquidus temperature.
As in Piombo and Dragoni ([56]) we adopt for K a temperature dependence

$$K(T) = K_0 e^{b/T} \tag{4.8}$$

where K_0 and b are constants.
In the model we adopt the parameter in tab. 4.2. The temperature decreases with time while the viscosity increases and then the flow slows down and the pressure on the barrier decreases. In this case the loss of pressure is not so relevant to modify the size of barrier structure. On the contrary a great difference in the barrier size can be using the rheological model as shown in figure 4.4. Such model need further calibration with experimental data to improve the lava-barrier interaction dynamics model description. For example, considering the power low behaviour of lava flow, the barrier dimension could be further reduced adopting the configuration in fig. 4.5.

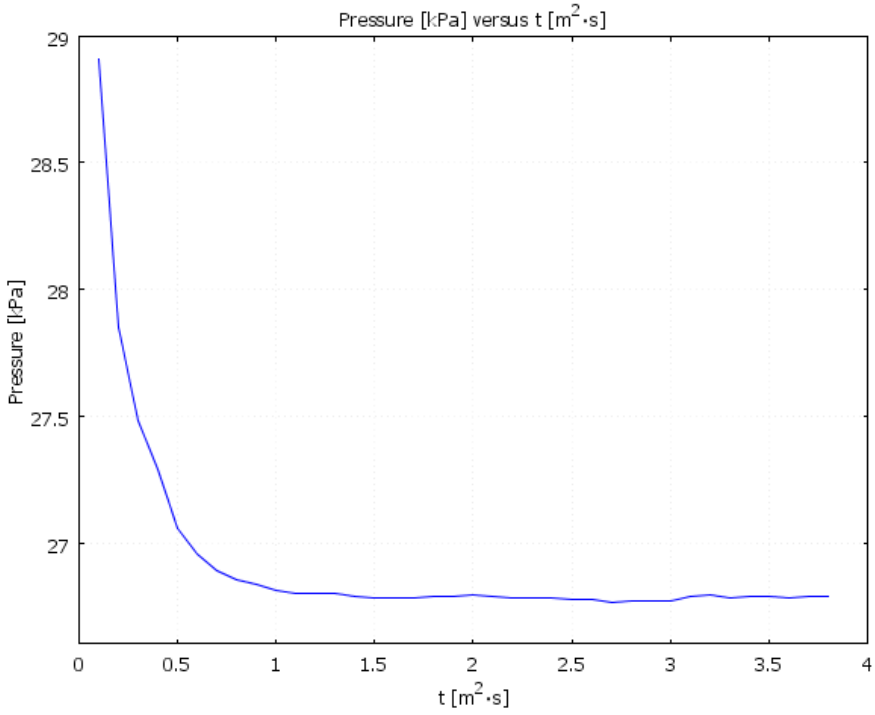

Figure 4.3: Pressure versus time on the lava barrier interface at one meter above the ground.

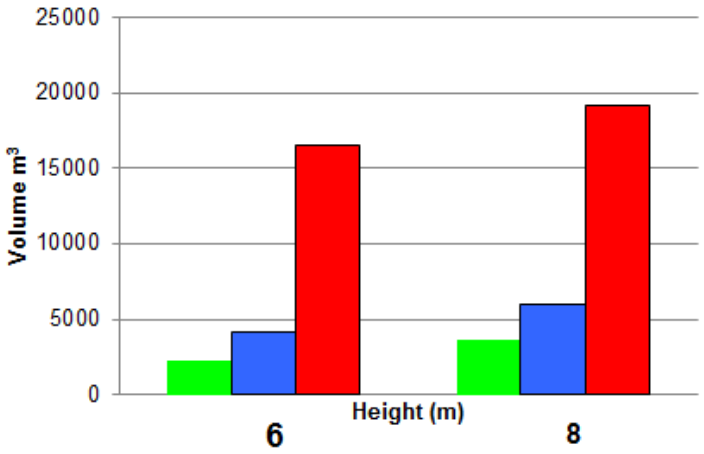

Figure 4.4: Comparison between volume necessary to build earth barrier during the 1983 emergency (in red), gabion barrier using 4.2 (in blue) and gabion barrier using rheological model (in green).

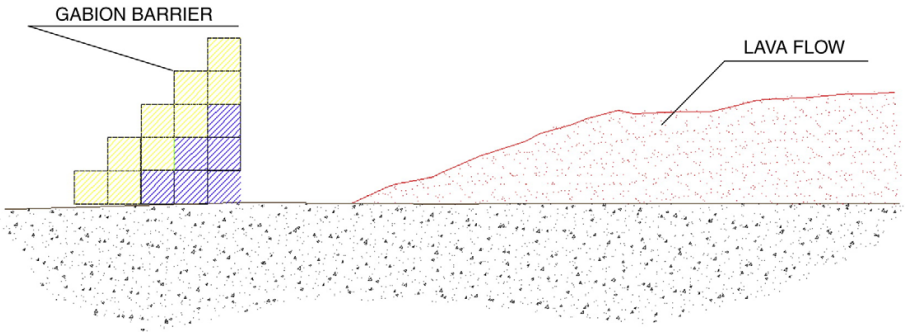

Figure 4.5: Hypothesis of a gabion barrier without positioning gabions in the upslope side.

4.4 Considerations on the operational aspects

4.4.1 Design of an earthen barrier

In the scientific literature there are very few example of studies describing the problem of barrier construction in volcanic areas.
Colombrita ([18]) described the methodology for the construction of earthen barriers at Etna. He considered the planning of earthworks developing in two phases:

- Defining of the optimal location for the works;

- Defining the geometrical characteristics of the works.

The aim of an earth barrier is to guide lava flows towards preselected zones so as to protect other zones of greater importance. The site of the works depends on the topography of the area that should be describe by up-to-date map at 1:5000 or 1:10000 scale. An earth barrier must have geometric characteristics that do not break under the pressure of the lava flows, and must be build in such way as to allow for any future rises in height. A barrier can be raised in two different ways: by pilling on material from above or by pushing material up from below. It is implied that the upper surface of the barrier should be at least 10 m wide in order to give trucks room to unload and bulldozers to spread the material. With a width less than 10 m the unloading speed is considerably reduced due to the congestion of vehicles. For the raising of a barrier from below, the escarpment facing the direction to be protected should have a slope of not more than 60% so as to allow the bulldozers and tracked power shovels to run along pushing up material at an appropriate rate. The other escarpment may have the same slope angle as the natural slope. An earth lava barrier is similar to the traditional one used in road building. However there are some aspects typical of this kind of work. One important difference between the geometry of a road embankment and barrier is the gradient and the access of the road. This requires a precise preliminary study of the sites and above all of the access roads in order to allow the vehicles to move around fully loaded. The problem consists in making an access road system with maximum gradients of 10% for erecting works having a gradient generally greater than 15% (in the Etna case, 16% to 20%). It is impossible to complete works of this kind in a very short time if the above considerations do not receive the due

amount of attention, it is in fact essential for achieving acceptable production rates in unloading and in quarries that the traffic on the sites moves without problems and at a fast speed. Another important aspect is the gradient of the road on top of the embankment. Generally, in its final stage, this road has a projected gradient equal to the natural one on the ground and is built in steps (one for each tip) having a gradient not greater than 10% in order to allow the unloading and shifting of material to occur in conditions of safety. This means that when the unloading process is completed, the embankment is of varying height. The irregularities can be smoothed out by bulldozers, but this is not advisable if it is foreseen that the height of the barrier may have to be raised. In addition, by not smoothing out the top, spare material that can be used in emergencies is available on site. However, all this must be considered at a planning stage, because the transport of a greater amount of material is involved which affects the construction time required.

4.4.2 Comparison between earthen and gabion barriers

From the analysis of past cases it is clear that barriers were generally constructed by building up earth, lava blocks and incoherent, low density material (scoria, lapilli and ash) to form containing walls. This solution implies complex operational constraints and logistical problems that justify the effort of looking for alternative design, derived from various fields of engineering applications. In particular, the set up of an earthen barrier, though very simple, requires a large amount of materials to be transported and, as a consequence, many working hours and heavy engineering vehicles which are able to push large quantities of soil. During the 1983 Etna eruption 18 days were necessary to build an earth barrier long 580 m and heigh 18 m using a mean of 10 bulldozers, 17 power shovels and 51 drumptrucks ([18]. A key point is therefore the reduction of the time necessary to erect the barrier. A second crucial aspect to be considered is the geometry of the barrier which is one of the few parameters that can be modulated while the others are linked to the morphological and topographical characteristics of the ground. Once the walls have been erected, the height of the structure may need to be increased. Unfortunately, if the barriers are made of incoherent material, it may be very difficult to increase their height as happened, for example, on Etna in 1992 when the top surface of an earthen barrier built up in Val Calanna was destroyed

by heavy rain making impossible to extend it vertically. Finally, in many cases, the operational and technological requirements must be planned in compliance with environmental and land planning restrictions, such as for Mt. Etna which is a protected natural park. For these reasons, methods for reducing and/or minimizing the impact of the built-up structure after the end of the eruption should also be investigated. The use of gabions has many advantages over loose riprap, such as earthen walls, owing to their modularity and capability of being stacked in various shapes. Furthermore, the elements which are not inundated by lava can be removed and used rapidly for other barriers. The gabions also have advantages over more rigid structures because they can conform to ground movement, dissipate energy from flowing water and drain freely. Their outer and inner faces may be straight or steeped. Walls can be built to increase resistance to overturning and the size and shape of each element should be proportioned in order to achieve internal stability. Wall heights can be increased by adding and interlocking new elements taking into account the wall's sensitivity to transverse differential settlement and preventing support of surcharge loads. Moreover, the volume of material necessary to build a gabion barrier is less than that of an earth barrier of the same height (fig.4.4). The barrier volume could be further reduced considering that the gabions positioned in the upslope side may not be necessary for the wall stability (fig.4.5). Thus fewer vehicles would be necessary to move the material. Finally, the material for filling the gabions can be extracted from a quarry that are distributed around all the volcano flank (fig.4.6) without creating the problem of where to obtain it, thus respecting the protected natural area. To verify the stability of the gabions during the transport an experimental test was carried out in June 2011. A number of gabions made available by Maccaferri S.p.a. were filled with volcanic rocks taken from a quarry located in Nicolosi (Etna south) (fig.4.8). The gabions were equipped with steel cables for the transport as showed in figure 4.7. In order to evaluate the deformation during the transport and placement the gabions were moved with a bulldozer. It resulted that the gabions can be moved easily once filled, without large deformations.

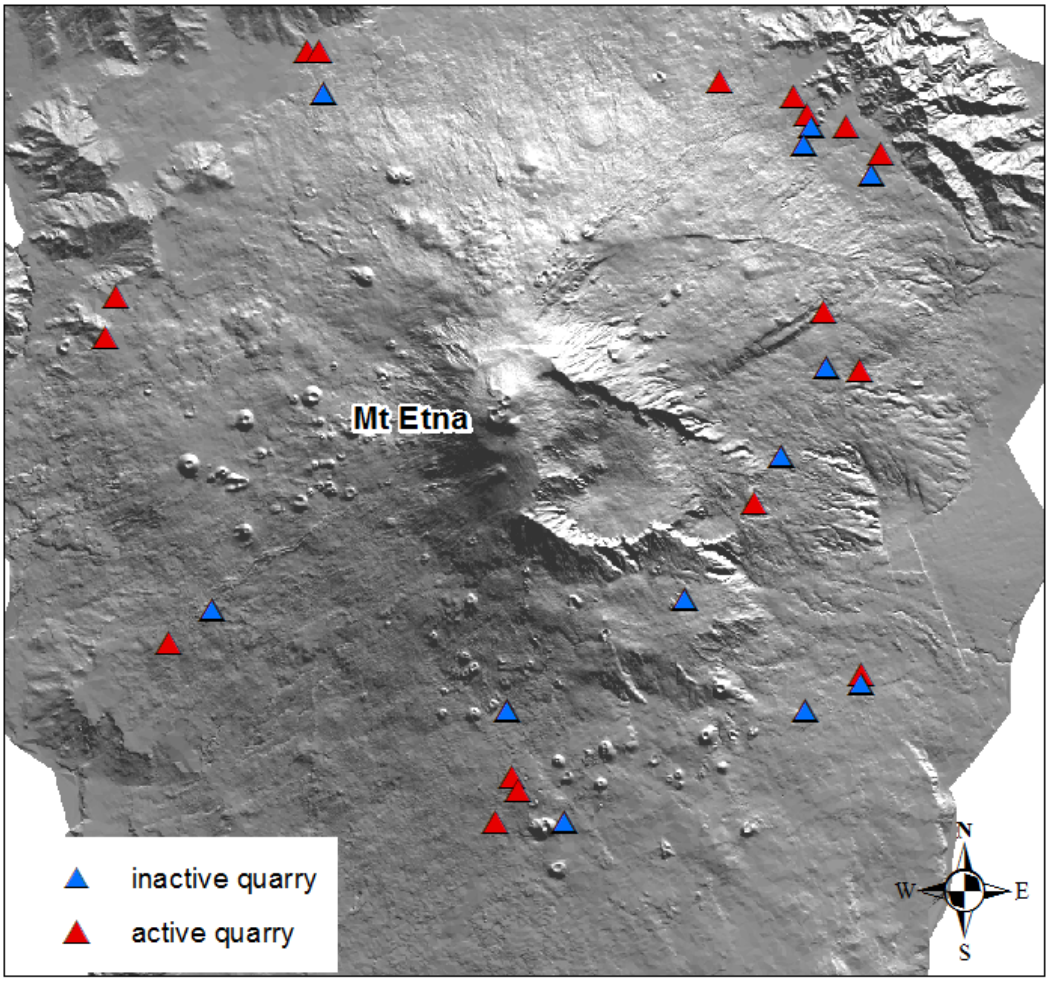

Figure 4.6: Inactive and active quarry around volcano flank where the material for filling the gabions can be extracted.

Figure 4.7: Phases of gabions assembly.

Figure 4.8: Experimental test: filling of the gabions stacked on top of each other.

Figure 4.9: Expetimental test: the gabions are moved once filled without large deformations.

Earthen barrier	Gabion barrier
Upper surface of the barrier should be at least 10 m wide	It is not necessary
The escarpment facing the direction to be protected should have a slope of not more than 60%	It is a step structure which allows to use less volume
Access road is necessary for both trucks and bulldozer	Access road could be necessary only for trucks, or could be not necessary if the gabions can be transported with helicopters
Long time to build a barrier	Short time respect to the earthen barrier if the gabions are filled
Distance between quarry and site influence the production rate	The gabions are filled in quarry and positioned in sensitivity areas around the volcano
Difficult to increase in height	It is possible to increase the height thanks their modularity
Hard-working to remove the not inundated material	the elements which are not inundated can be easily removed

Table 4.3: Comparison between earthen and gabion barrier.

Chapter 5

Modeling and simulation

The TADR trends can be used as input for simulation models that are adopted for evaluating different scenarios of volcanic hazard. Furthermore, they represent a constrain to understand the eruptive mechanism of the eruptions that can be used to foresee the behaviour of lava flows.
This chapter illustrates examples of the use of TADR trend for both applications. In particular, we investigate first how the numerical simulations can be adopted for evaluating different scenarios of volcanic hazard and the effectiveness of a barrier configuration. Then, starting from the analysis of TADR trend of 1981 Etna eruption we propose an eruptive mechanism.

5.1 Lava flow simulation for evaluating mitigation actions

Numerical simulation codes provide a powerful tool in testing the effectiveness of these mitigation actions. As a matter of fact the simulated lava path can be used to define an optimized project to locate the work. Simulation codes were applied in few cases to understand the effect on lava flow path of artificial barriers for hazard mitigation. The first phase of the 1991-1993 Etna lava flow has been simulated using a probabilistic code ([26]). The results of human interventions, such as the

construction of a barrier at Portella Calanna and lava flow diversion by obstructing the lava tunnel in Valle del Bove, were evaluated. During the 2001 Etna eruption, simulations by the SCIARA code ([9]) were carried out to reproduce the main flow propagation and, varying the flow rates, to forecast possible scenarios.When simulations showed that lava flows threatened inhabited areas, morphology alterations were introduced to reproduce possible operations to deviate the lava flow ([23]). The LavaSIM code ([42]) was adopted to evaluate the effects of artificial barriers, water-cooling and guiding channels on 1986 Izu-Oshima lava flow, providing quantitative results useful for real-time crisis management ([33]). Finally, the DOWNFLOW code was adopted to investigate the possibility of reducing the lava flow hazard at Nyiragongo volcano, particularly for the neighboring towns of Goma (DRC) and Gisenyi (Rwanda), by modifying the pre-eruption topography for simulating the construction of protective barriers ([17];[30]; [29]). In this study the barriers built during the 2001 Etna eruption to protect zones under significant threat were selected as test case and we adopted the MAGFLOW code, developed at INGV Sezione di Catania.

5.1.1 The MAGFLOW code

The MAGFLOW code, developed at INGV Sezione di Catania, is a Cellular Automata (CA) model for simulating the lava flow emplacement ([25]; [77]). In MAGFLOW the state of the cells is defined by the lava thickness and the quantity of heat. Its evolution function is the steady-state solution of Navier-Stokes's equation for the motion of a Bingham fluid, subject to pressure force, on an inclined plane. In order to reduce the impact of the cell geometry, a Monte Carlo approach was adopted to improve the solution ([77]). The simulation starts discharging lava at a certain rate from one or more vent cells as a function of the flow rate that can change over time, thus increasing the lava thickness at the vents. When such thickness reaches a critical level, the lava spreads over the neighbouring cells. Next,whenever the thickness at any cell exceeds the critical thickness, the lava flows into its neighbours. At the same time, the heat content of the lava in each cell is modified in accordance with the flow motion and by considering the heat loss by radiation from the flow surface; solidification effects are also modelled. The code was quantitatively validated by simulating the whole emplacement of

Parameter	Value
Density of lava	2700 kg/m^3
Specific heat	1150 J/kgK
Lava emissivity	0.9
Solidification temperature	1143 K
Temperature of extrusion	1360 K

Table 5.1: Physical and rhelogical lava properties

the main 2001 Etna lava flow ([20]; [77]). It was also applied to the 2006 Etna lava flow allowing to investigate different viscosity laws to be implemented in the code, and a methodology for satellite estimation of the effusion rate ([25]; [77]).

5.2 Simulation test: the 2001 Etna eruption

The simulations of the lava flow emplacements from the 2700 m and 2550 m a.s.l. vents were run using the MAGFLOW code for different scenarios: one in which the pre-eruption topographic surface include the barriers (real case) and two corresponding to different barrier configurations. Physical and rheological properties of the lava ([77]) are listed in table 5.1 while the TADR trends of the two flows are described in chapter 2.
First test simulated the real event because it was run on the pre-eruption DEM modified to include the thirteen barriers built during the eruption. The second test simulated the path the lava would have naturally followed without human intervention because it was run on the pre eruption DEM without the barriers. Finally, the third test simulated an alternative intervention because it was run on the pre-eruption DEM which included a barrier built in a position different from that of the actual barriers.

5.2.1 Results validation

The MAGFLOW code and the input parameters to be adopted for the 2001 Etna eruption had already been validated versus the main lava flow ([59]; [77]). The same approach have been here adopted on the results of the first simulation in order to check the reliability of the reconstruction of the two emplacement

histories by comparing the real and simulated flow spreads. A first comparison was based on the analysis of overestimated, underestimated and overlapping areas. The overestimated area is that covered by the simulated flow but not by the real one, the underestimated area is that covered by the real flow but not by the simulated one, and finally the overlapping area is that covered by both the real and simulated flows. When comparing the simulated flow field to the real one (fig. 5.1), we observe that the results underestimate the flows in the first two days of the eruption (18 and 19 July 2001) (fig.5.2) later the simulation provides overestimated simulated areas and (fig.5.3), finally, the two areas appear almost completely overlapped (fig.5.4). Then a quantitative validation of the results

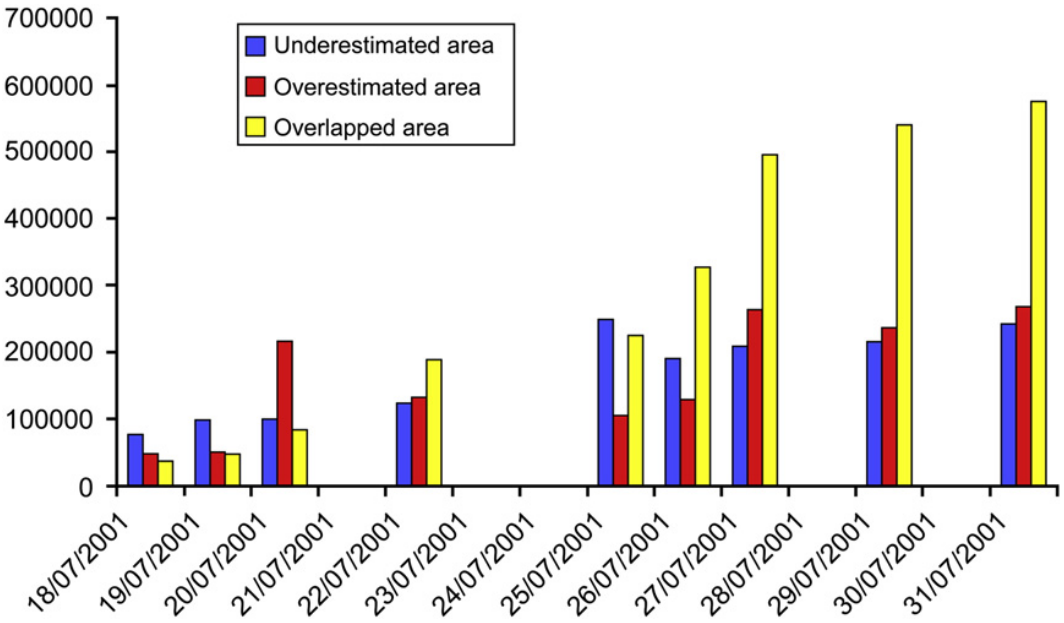

Figure 5.1: Differences between observed and simulated lava flow area at all the simulation dates; in blue, red and yellow underestimated, overestimated and overlapping areas, respectively.

was based on the joint analysis of the percent length ratio (PLR), which allows to verify the correspondence between simulated and observed lengths ([60]), and the fitness function adopted to quantify the matching between simulated and observed areas ([70]). These two parameters are defined as in equation 5.1 and 5.2.

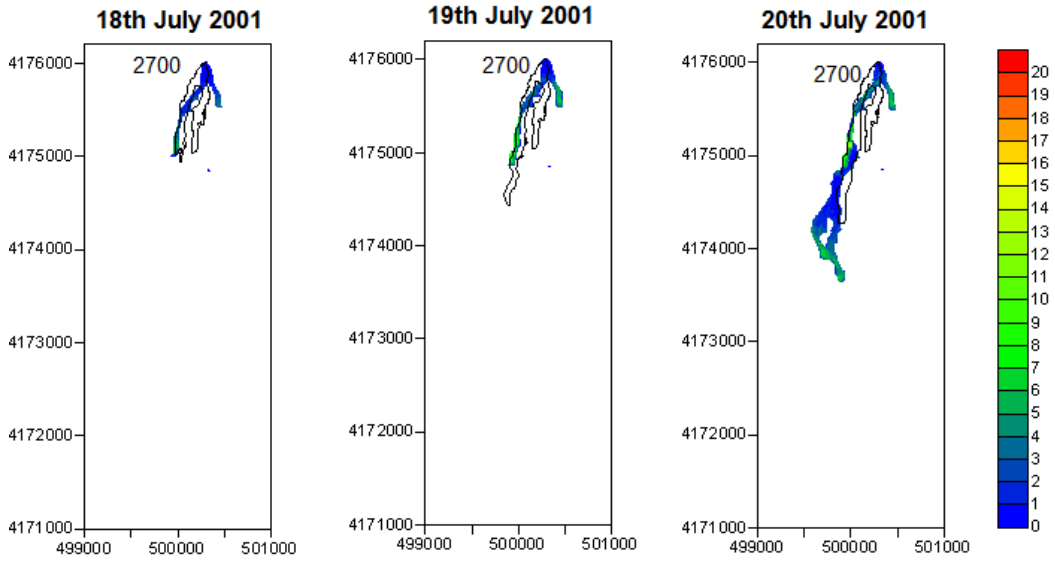

Figure 5.2: Comparison between the simulated (color scale) and real 2001 lava flows (black lines) from 18th to 20th July 2001

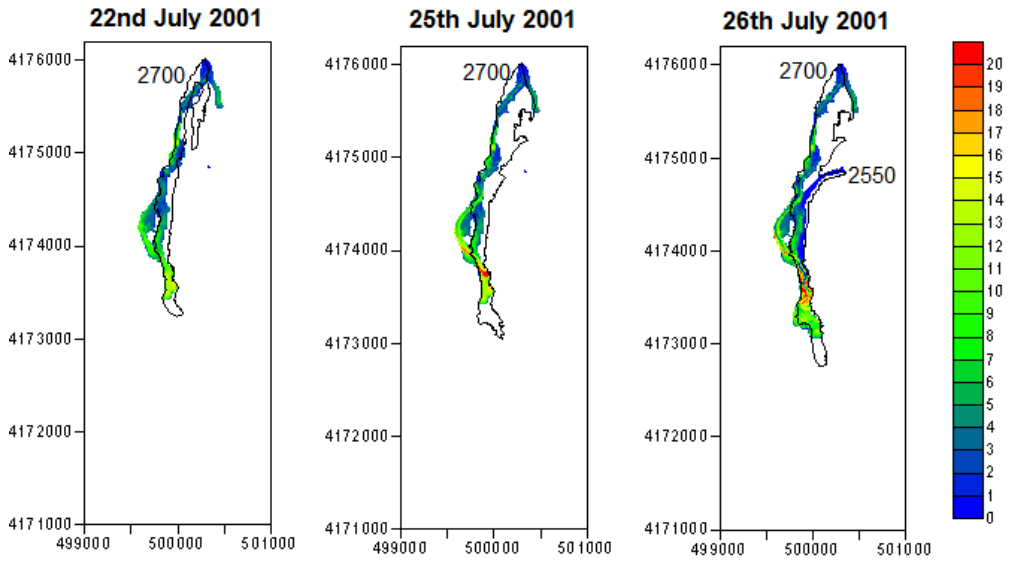

Figure 5.3: Comparison between the simulated (color scale) and real 2001 lava flows (black lines) from 22nd to 26th July 2001

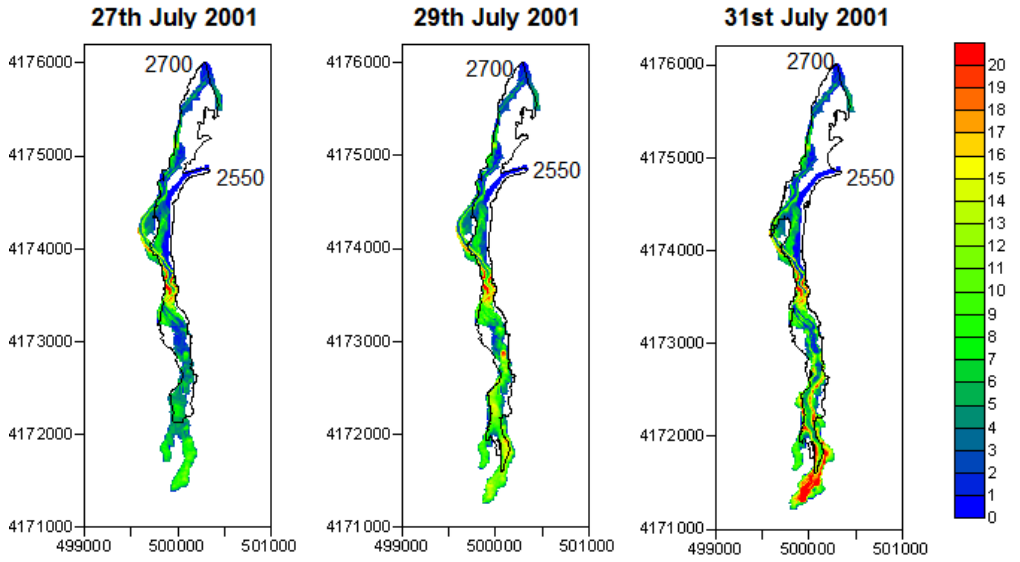

Figure 5.4: Comparison between the simulated (color scale) and real 2001 lava flows (black lines) from 27th to 31st July 2001

$$PLR = \frac{L_{sim}}{L_{obs}} \cdot 100 \tag{5.1}$$

where L_{sim} and L_{obs} are, respectively, simulated and observed length measured along the main direction of the flow.

$$e_1 = \sqrt{\frac{mR \cap S}{mR \cup S}} \tag{5.2}$$

where m(A) denotes the measure of the region A, while R and S are the areas affected by the real (observed) and simulated event. $R \cup S$ is, here, the sum of underestimated, overlapping and overestimated areas while $R \cap S$ is the overlapping area.

5.2.2 Discussion of results

Figure 5.5 shows a quite good fit between simulated and real flows on 22, 25 and 27 July and a good fit between simulated and real flows on 26, 29 and 31 July. Because the lava flows approached the earth barriers and the Rifugio Sapienza on

25 and 26 July we obtained a good reproducibility of the flow advancement in the more interesting area and thus the code can be adopted for further studies on alternative barrier building. The differences between the first simulation and the

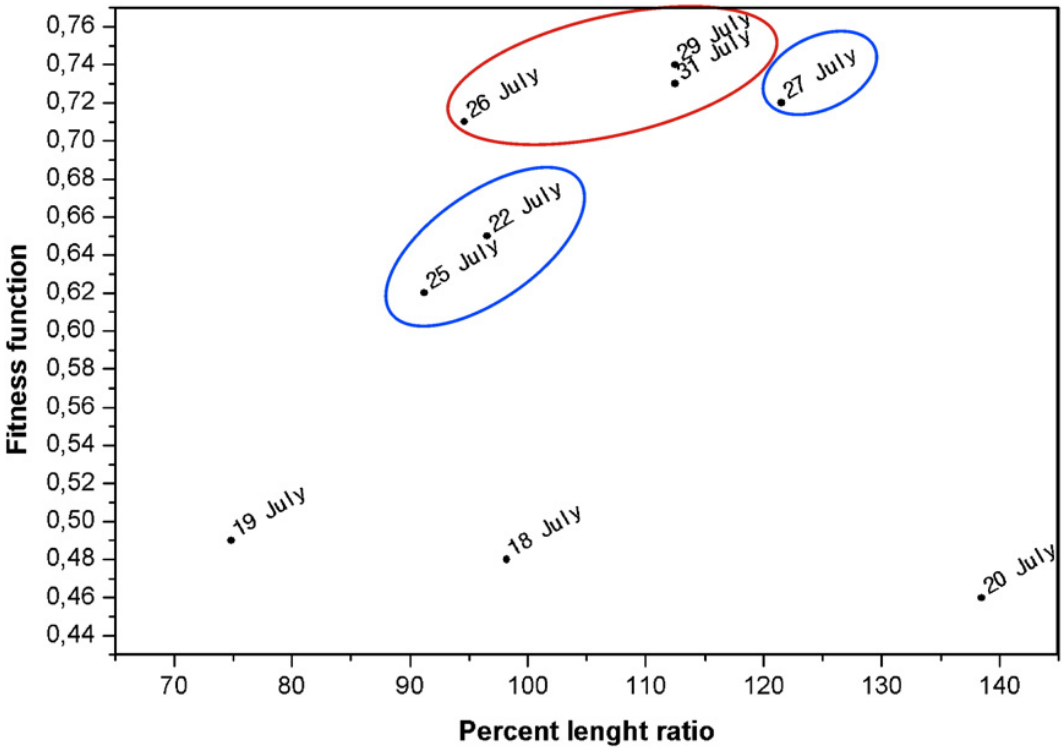

Figure 5.5: Fitness function (e_1) versus percent length ratio (PLR) for all the simulation dates. Blue ellipses delimit the dates (22, 25 and 27 July) corresponding to a quite good fit between simulated and real flows; red ellipse delimits the dates (26, 29 and 31 July) corresponding to a good fit between simulated and real flows.

observed flow emplacement, mostly observed in the first days, derive from artefact in the DEM resulting from data interpolations, from the difficulties in delimiting the covered areas and in reconstructing the daily thickness's and thus in estimating the effusion rates, and finally from some approximation in the MAGFLOW modeling of the lava's rheological behaviour and/or cooling process [77]. It should also be evidenced that the pre-eruption DEM has a quite low resolution (cell dimension 10 m), which was comparable with the width of the flow branches (10-20 m) during the first days of the eruption. This caused the simultaneous activation of too many cells and resulted in higher lateral lava spreading, thus promoting the

lava propagation along the maximum slope direction and causing the formation of a secondary branch toward south-west that was poorly fed until 26 July. Moreover, data interpolation by TIN (Triangular Irregular Network) method can create topographic artefacts and, in particular, flat areas which can influence the simulated flow path and also cause its diversion from the real one. The small-scale variations, characterizing the Mt. Etna complex morphology, may be neglected when interpolating the pre-eruption surface from contour lines. Such variations hold relevant importance mostly on the first emplacement phase, when the lava thickness is low and comparable with the height difference between adjacent grid cells. A better result could be obtained from the editing of the pre-eruption DEM, for example, for removing flat areas that had been generated during TIN interpolation.

5.2.3 Effectiveness of barrier configurations

After assessing the reproducibility of the actual flow evolution by the MAGFLOW code, the influence of the barriers on the lava spreading can be investigated, in particular upper slope the Rifugio Sapienza area (fig. 5.6). We should note that, in the first simulation, the presence of the B1, B2 and B3 barriers represented an obstacle to the advance of the lava flow, and the simulated flow was characterized by an increment of thickness in correspondence of them (fig. 5.6a and b). The second simulation demonstrated that, without the building of the barriers, the lava would have covered the tourist facilities of the Sapienza zone, whereas in the real case the structures were protected by the C4 barrier (fig. 5.6 c and d). Moreover, in the second simulation it is evident the lack of the above mentioned increment of thickness close to the B1, B2 and B3 barriers, clearly recognizable in the simulation of the actual flow emplacement (fig. 5.6 a and b). Such difference is a further support to the effectiveness of these barriers in slowing down the lava flow and for demonstrating that the MAGFLOW code is sensitive to small variations of the elevation. The last simulation proposed an alternative positioning and dimensioning of the C4 barrier, the barrier N, which would be higher (15 m) and longer (390 m) (fig. 5.7 e). In this test, a single barrier was used to successfully protect the facilities of the Sapienza's zone that were not buried.

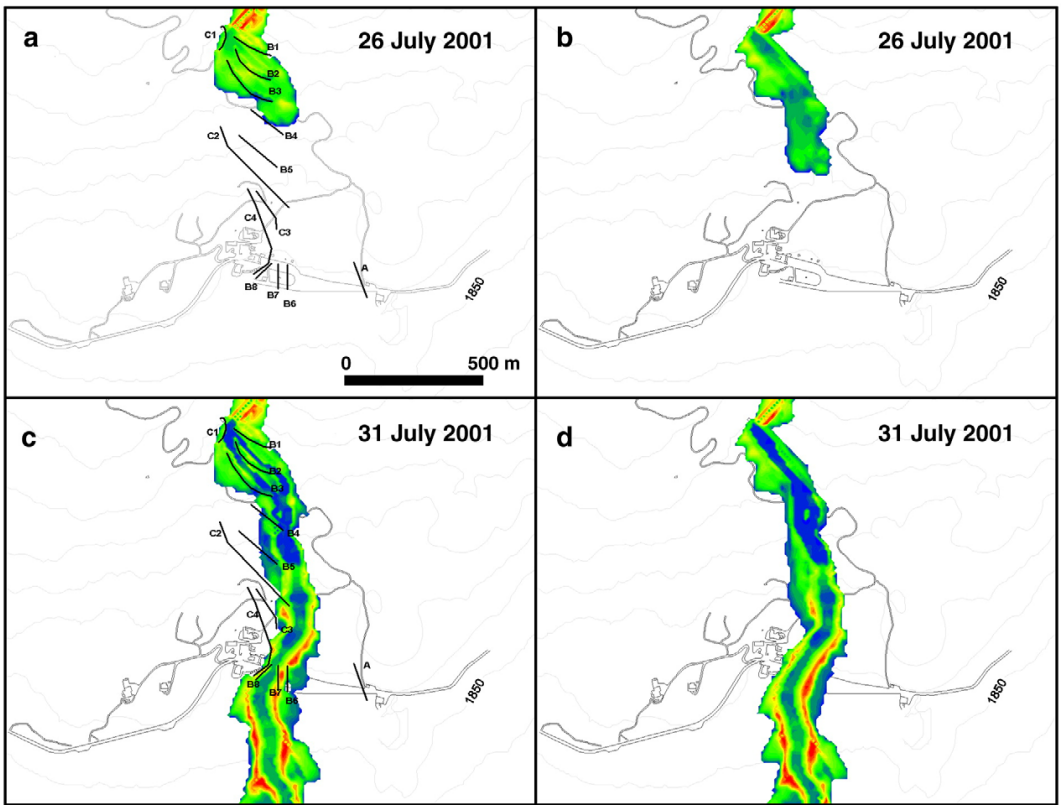

Figure 5.6: Simulated flow thickness upslope the Rifugio Sapienza area obtained from: (a) the first simulation reproducing the real case (run above the pre-eruption DEM plus the 2001 actual barriers); (b) the second simulation, reproducing the path the lava would have naturally followed without the human intervention (run above the pre-eruption DEM without the barriers). Simulated flow thickness upslope, close to and downslope the Rifugio Sapienza area obtained from: (c) the first simulation; (d) the second simulation

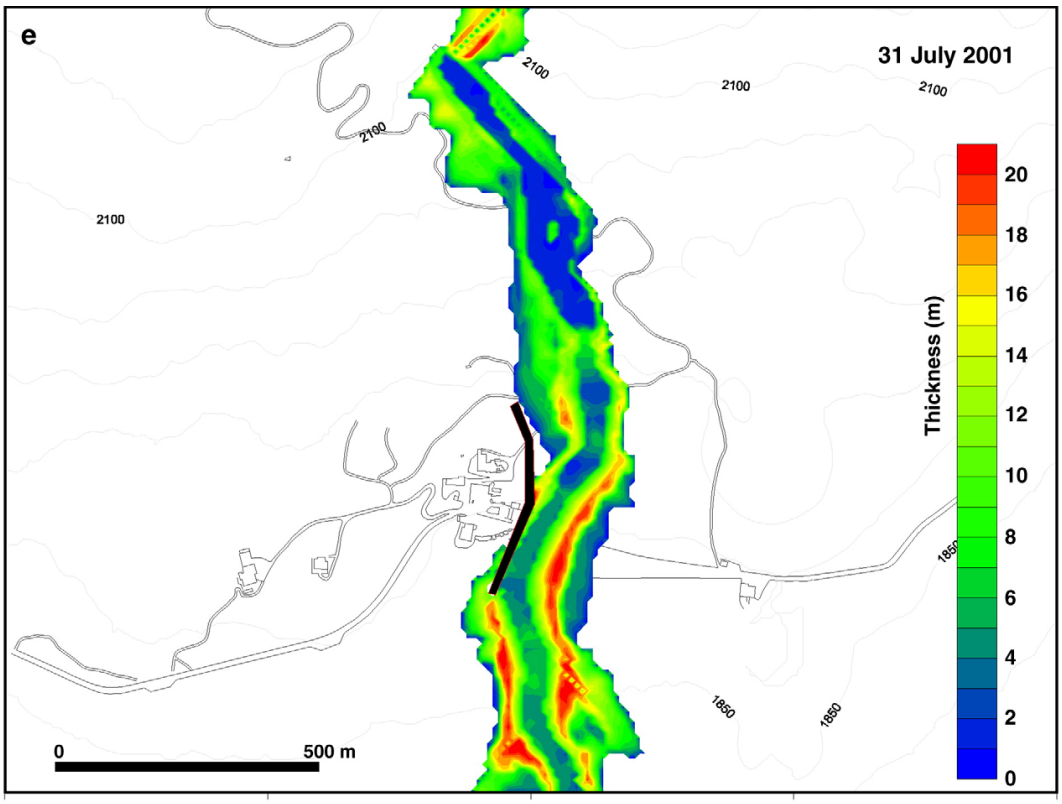

Figure 5.7: (e) The third simulation, representing an hypothetical case (run above the pre-eruption DEM, modified to include an hypothetical barrier located in a different position from those really built). Scale bar reported in a refers to a, b, c and d; color scale reported in e refers to all the maps showed in this figure.

5.3 Simulation test: the 1981 Etna eruption

The 1981 Etna eruption was characterized by a very fast evolution of lava field. Simulation tests were used to show different scenarios of volcanic hazard. The input data are the pre-eruption topography, the TADR trend, the rheological characteristic of lava (tab. 5.1) and the vents position. The first simulation represents the real event to verify the capability of the simulation code to model fast evolution lava flow. The second simulation shows what would have happen if the main lava flow had been released from the lowest vent opened the last days of the eruption. Usually the lowest point of the crack is characterized by the highest emission rate. Thus these simulations we consider that the lowest fissure emitted the volume of the main flow at a constant rate (fig. 5.9) and at a variable effusion rate (fig. 5.10). Both simulations showed that in a very short time Randazzo would have been completely covered. In such situation it is impossible to build a barrier system during the eruption and only a pro active interventions should be considered. For example permanent barriers or road embankments taking advanced of the topography of the area can be a priori built up to protect selected valuable areas.

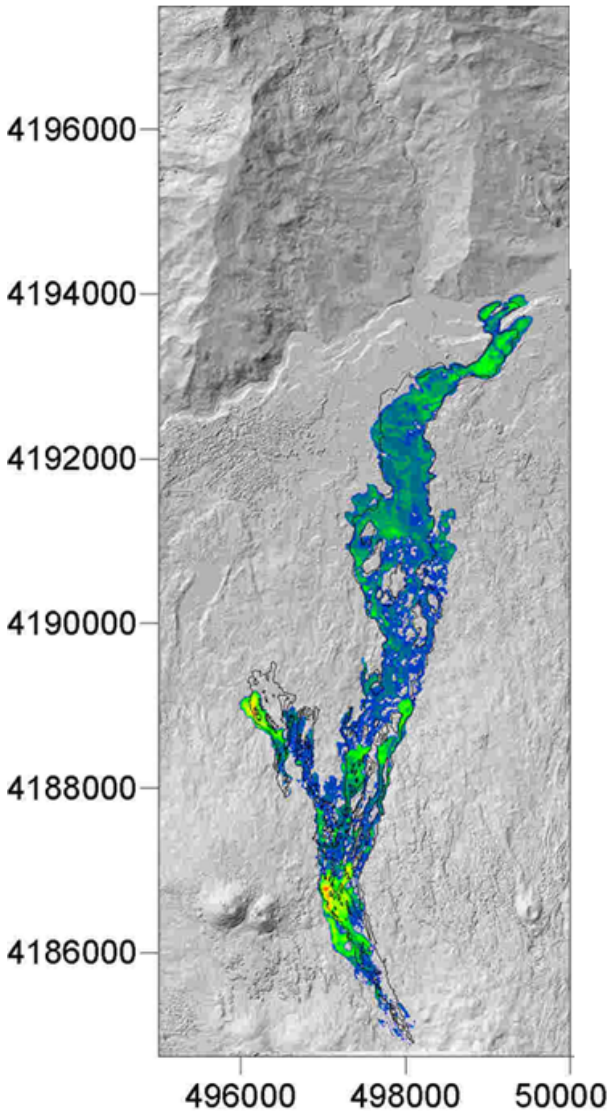

Figure 5.8: The simulation reproduces the real case, run above the pre-eruption DEM

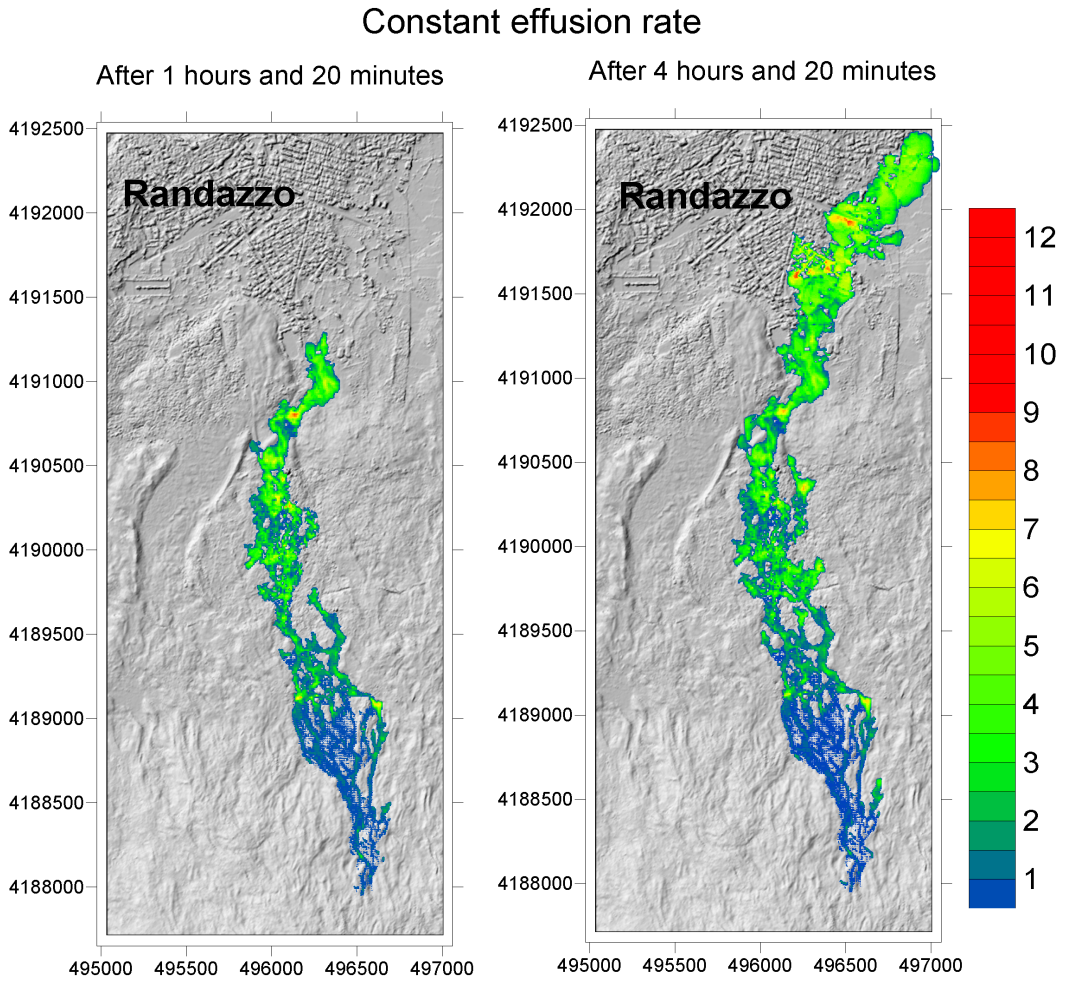

Figure 5.9: The simulation shows the simulated lava flow field if the lowest vent would emitted the volume of the main flow with constant effusion rate

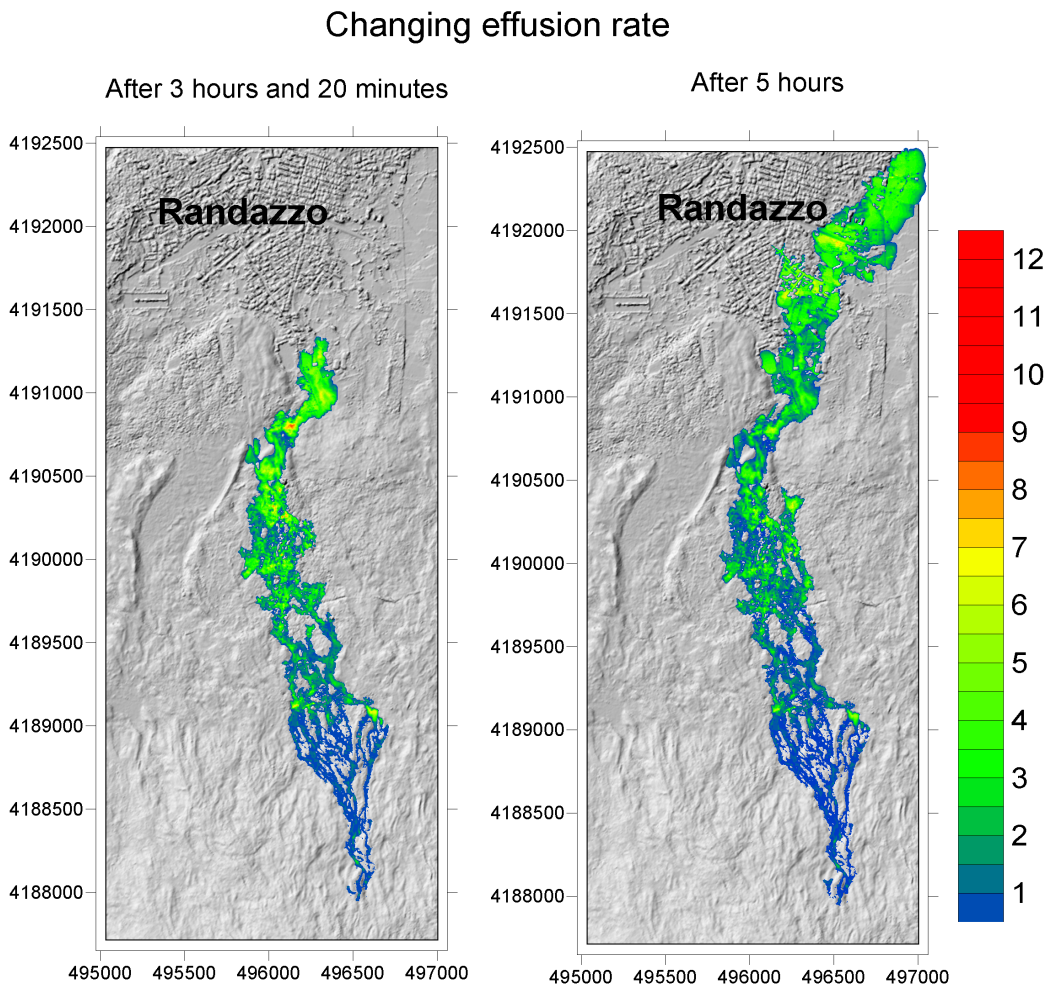

Figure 5.10: The simulation shows the simulated lava flow field if the lowest vent would emitted the volume of the main flow with changing effusion rate

Chapter 6

Conclusions

A quantitative analysis of an eruption evolution based on the reconstruction of the TADR trend and of the related hazard assessment analysis represents an important improvement in volcanology. It permits the evaluation of the most efficient mitigation actions and supports lava flow simulations, also contributing to the understanding of eruptive mechanisms. The temporal evolutions of the 2001, 1981 and 1928 Etna eruptions were reconstructed and the TADR trends were estimated using a quantitative approach. The analysis was based on lava flow evolution maps and lava thickness' maps evaluated as the difference between pre- and post-eruption DEMs. The study has evidenced that some flank eruptions of Mt Etna can reach very high effusion rates, like for example in the 1928 and 1981 eruptions when the maximum values of TADR exceeded 600 m^3/s. Such high values should be taken into account by the civil protection because they highlight the necessity to reduce the intervention time to carry out mitigation actions.
The TADR analysis was taken as a starting point for investigating discharge mechanisms of not very well known fast flowing flank eruptions. The main achievement of the work is understanding of the rapid evolution of the 1981 main flow attributed to a sudden emptying of a shallow magma reservoir interacting with a dike intrusion from the deeper part of the plumbing system.
Furthermore, the TADR trends furnish the input parameters to simulate the evolution of the lava flows and to forecast different scenarios of volcanic hazard. Simulations were conducted for the 1981 and 2001 eruptions reproducing both the real events and different scenarios useful for volcanic hazard assessment. Due to the

fast evolution of the 1981 eruption, the simulation showed that in few hours the city of Randazzo would have been covered if the lowest portion of the fissure had presented the highest discharge rate. In similar cases active mitigation measures are very hard to be realized while pro-active interventions might be considered. For the 2001 eruption, the analysis of the lava thickness distributions, resulting from the three simulations, demonstrates the effectiveness of the barriers in slowing down the lava flow. In addition, to optimize the barrier construction a gabion structure was proposed. In this way the volume of material to be transported is reduced with respect to earthen barriers and the time necessary to erect the structure becomes significantly shorter. The availability of a number of gabions, previously filled and stocked in strategic sites, permits to built up an efficient barrier following a detailed plan based on the flow simulation results. This approach improves the effectiveness of civil protection interventions during the emergencies.

Acknowledgments

I would like to express my sincere acknowledgement to my professor Maria Marsella for providing me an opportunity to carry out my research. Her support and friendship has been invaluable on both an academic and a personal level, for which I am extremely grateful.
I am most thankful to Dr. Mauro Coltelli for his good advice and help concerning the volcanology aspects of my research and for his constant encouragement.

I also thank,
Prof. Quintilio Napoleoni, for his help and advice in the engineering aspects of this Phd work,

Dr. Ciro Del Negro and Dr. Anna Vicari, for their availability in carrying out all necessary things in the simulation phase,

Prof. Michele Dragoni and Prof. Andrea Tallarico, for the helpful discussions during the modelling phase,

Prof. Paolo Baldi, for providing me with the photogrammetry tools,

Dr. Salvo Caffo, for his helpfulness and constant interests he showed towards this research work.

I would also like to thank my fellow research group and friends, in particular Cristina Proietti for her valuable assistance during our missions in Sicily and for her kind collaboration during the Phd works, Peppe J.V. D'Aranno for his contribution in lava flow reconstruction and Alberico Sonnessa for his help and

friendship.

Above and beyond all, my heartfelt gratitude to my father Enzo, my brother Daniele and friends (Erika, Laura, Valeria, Luisa, Valentina, Laura, Veronica, Giulia, Maria Rita) for their much needed support, patience, understanding, and encouragement in every possible way.

Bibliography

[1] *Gawacwin software.*

[2] *SOCET SET - User's Manual.*

[3] *Photogrammetry.* Dummlers Verlag., 1997.

[4] L. Abersten. Diversion of a lava flow from its natural bed to an artificial channel with the aid of explosive etna 1983. *Bull. Volcanol.*, 1984.

[5] P. Allard, P. Baxter, M. Halbwachs, and J. C. Komorowski. Final report of the french-british scientific team. the january 2002 eruption of nyiragongo volcano (dem. repub. congo) and related hazards: observations and recommendations. *Reporto of Ministry for Foreign Affairs, Paris, France*, 2002.

[6] F. Barberi, F. Brondi, M.L. Carapezza, L. Cavarra, and C. Auriga. Earthen barriers to control lava flows in the 2001 eruption of Mt. Etna. *J. Volcanol. Geoth. Res.*, 2003.

[7] F. Barberi and M.L. Carapezza. The control of lava flow at mount etna. *Mount Etna Volcano Laboratory. : Geophysical Monograph Series*, 2004.

[8] F. Barberi, M.L. Carapezza, M. Valenza, and L. Villari. The control of lava flow during the 1991-1992 eruption of mount etna. *J. Volcanol. Geoth. Res.*, 1993.

[9] D. Barca, G.M. Crisci, and R. Rongo. Application of the cellular automata model sciara to the 2001 mount etna crisis. *Mount Etna Volcano Laboratory: Geophysical Monograph Series*, 2004.

[10] B. Behncke, M. Neri, and A. Nagay. Lava flow hazard at mount etna (italy): new data from a gis-based study. *Geological Society of America*, 2005.

[11] A. Bonaccorso. The march 1981 mt. etna eruption inferred through ground deformation modelling. *Physics of the Earth and Planetary Interiors*, 1999.

[12] S. Branca and P. Del Carlo. Eruptions of mt etna during the past 3,200 years: a revised compilation integrating the historical and stratigraphic records. *Mount Etna volcano laboratory, Geophysical Monograph Series*, 2004.

[13] S. Branca and P. Del Carlo. Types of eruptions of etna volcano ad 1670-2003: implications for short-term eruptive behavior. *Bull. Volcanol.*, 2005.

[14] S. Calvari, M. Coltelli, M. Neri, M. Pompilio, and V. Scrivano. The 1991-1993 etna eruption : chronology and lava flow-field evolution. *Acta. Volcanol.*, 1994.

[15] D. Carbone, G. Currenti, and C. Del Negro. Multiobjective genetic algorithm inversion of ground deformation and gravity changes spanning the 1981 eruption of etna volcano. *J. Geophys. Res.*, 2008.

[16] C. Chiarabba, P. De Gori, and D. Patané. The mt. etna plumbing system: the contribution of seismic tomography. *Mount Etna volcano laboratory, Geophysical Monograph Series*, 2004.

[17] G.D. Chirico, M. Favalli, P. Papale, E. Boschi, M.T. Pareschi, and A. Mamou-Mani. Lava flow hazard at nyiragongo volcano, drc 2. hazard reduction in urban areas. *Bull. Volcanol.*, 2008.

[18] R. Colombrita. Methodology of the construction of earth barriers to divert lava flows the mt. etna 1983 eruption. *Bull. Volcanol.*, 1985.

[19] M. Coltelli, M. Marsella, C. Proietti, and S. Scifoni. The case of the 1981 eruption of mount etna, an example of very fast moving lava flows. *Geochem. Geophys. Geosyst.*, 2012.

[20] M. Coltelli, C. Proietti, S. Branca, M. Marsella, D. Andronico, and L. Lodato. Analysis of the 2001 lava flow eruption of Mt. Etna from 3D mapping. *J. Geoph. Res*, 2007.

[21] D. Coppola, D. Piscopo, T. Staudacher, and C. Cigolini. Lava discharge rate and effusive pattern at piton de la fournaise from modis data. *J. Volc. Geoth. Res.*, 2009.

[22] M. Cosentino, R. Cristofolini, M. Ferri, G. Lombardo, G. Patané, R. Romano, A. Viglianisi, and P. Villari. L'eruzione dell'Etna del 17-23 marzo 1981. rapporto preliminare. *Rend. Soc. Geol. It.*, 1981.

[23] G.M. Crisci, R. Rongo, S. Di Gregorio, and W. Spataro. The simulation model sciara: the 1991 and 2001 lava flows at mount etna. *J. Volcanol. Geoth. Res.*, 2004.

[24] P.J.V. D'Aranno. Analisi quantitativa dell'evoluzione di una colata storica dell'Etna, mascali 1928, per la valutazione di scenari di mitigazione del danno. Master's thesis, Sapienza University of Rome, 2011.

[25] C. Del Negro, L. Fortuna, A. Herault, and A. Vicari. Simulations of the 2004 lava flowat etna volcano by the magflowcellular automata model. *Bull. Volcanol.*, 2007.

[26] F. Dobran and G. Macedonio. Lava modeling contributions of the volcanic simulation group during the 1991-1992 eruption of mt. etna. *Volcanic Simulation Group Report*, 1924.

[27] A.M. Duncan, C. Dibben, D.K. Chester, and J.E. Guest. The 1928 eruption of Mount Etna Volcano, sicily, and the destruction of the town of mascali. *Disasters*, 1996.

[28] M. Favalli, G. D. Chirico, P. Papale, M. T. Pareschi, M. Coltelli, and N. Lucaya. Computer simulations of lava flow paths in the town of goma, nyiragongo volcano. *Journal of Geophysical Research*, 2006.

[29] M. Favalli, G.D. Chirico, P. Papale, M.T. Pareschi, and E. Boschi. Lava flow hazard at nyiragongo volcano, d.r.c. 1. model calibration and hazard mapping. *Bull. Volcanol.*, 2008.

[30] M. Favalli, M.T. Pareschi, A. Neri, and I. Isola. Forecasting lava flowpaths by a stochastic approach. *Geophys. Res. Lett.*, 2005.

[31] M. Filippucci, A. Tallarico, and M. Dragoni. A three-dimensional dynamical model for channeled lava flow with nonlinear rheology. *J. Geophys. Res.*, 2010.

[32] I. Friedlander. Der etna-ausbruch 1928. *Zeitschrift fÃ¼r Vulcanologie*, 1928.

[33] E. Fujita, M. Hidaka, A. Goto, and S. Umino. Simulations of measures to control lava flows. *Bull. Volcanol.*, 2008.

[34] Wadge G. The variation of magma discharge rate during basaltic eruptions. *Journal of Volcanology and Geothermal Research*, 1981.

[35] Wadge G. Retrieval of large volcanomagnetic effects observed during the 1981 eruption of mt. etna. *Annals of Geophysics*, 1997.

[36] D. Giordano and D.B. Dingwell. Viscosity of hydrous etna basalt: implications for plinian-style basaltic eruptions. *Bull. Volcanol.*, 2003.

[37] J.E. Guest, C.R.J. Kilburn, H. Pinkerton, and A.M. Duncan. The evolution of lava flow field : observation of 1981 and 1983 eruptions of mount etna, sicily. *Bull. Volcanol.*, 1987.

[38] H.C. Hardee and J.C. Dunn. Convective heat transfer in magmas near the liquidus. *J. Volcanol. Geotherm. Res.*, 1981.

[39] A. J. L. Harris, J. B. Murray, S. E. Aries, M. A. Davies, L. P. Flynn, M. J. Wooster, R. Wright, and D. A. Rothery. Effusion rate trends at etna and krafla and their implications for eruptive mechanisms. *J. Volc. Geoth. Res.*, 2000.

[40] A.J.L. Harris, J. Dehn, and S. Calvari. Lava effusion rate definition and measurement: a review. *Bull Volcanol*, 2007.

[41] C. Heliker and T. N. Mattox. The first two decades of the pu u oo-kupaianaha eruption: Chronology and selected bibliography. *U.S. Geological Survey Professional Paper*, 2003.

[42] M. Hidaka, A. Goto, S. Umino, and E. Fujita. Vtfs project: development of the lava flow simulation code lavasim with a model for three-dimensional convection spreading and solidification. *Geochem. Geophys. Geosyst.*, 2005.

[43] G. Imbó. Osservazioni e ricerche in relazlone all' eruzione etnea 2 - 20 novembre 1928. Technical report, R. Osservatorio Geofisico di Catania, 1929.

[44] INGV. Report 2002 etna eruption. Technical report, INGV, 2002.

[45] Smitsonian Institution. Scientific event alert network bulletin (1978-89). Technical report, Smitsonian Institution, 1989.

[46] C.R.J. Kilburn. Lava crusts, aa flow lengthening and the pahoehoe-aa transition. *Active Lavas: Monitoring and Modelling. UCL Press*, 1993.

[47] C.R.J. Kilburn. Fracturing as a quantitative indicator of a lava flow dynamics. *J. Volcanol. Geoth. Res.*, 2003.

[48] P. W. Lipman and N. G. Banks. Aa flow dynamics, mauna loa 1984. *Volcanism in Hawaii: US Geological Survey Professional Paper*, 1987.

[49] M. Marsella, S. Scifoni, M. Coltelli, and C. Proietti. Quantitative analysis of the 1981 and 2001 etna flank eruptions: a contribution for future hazard evaluation and mitigation. *Annals of Geophysics*, 2011.

[50] M. Maugeri and R. Romano. Suggestion for preventive and/or defensive works against lava flows in the etnean area. *Bull. B.R.G.M.*, 1980-1981.

[51] G.A. Mcdonald. Barrier to protect hilo from lava flows. *Pac.Sci.*, 1958.

[52] G.A. Mcdonald. The 1959 and 1960 eruptions of kilauea volcano, hawaii, and the construction of walls to restrict the spread of the lava flows. *Bull. Volcanol.*, 1962.

[53] M. Neri and V. Acocella. The 2004-2005 etna eruption: implications for flank deformation and structural behaviour of the volcano. *J. Volc Geoth. Res.*, 2006.

[54] A. Peltier, T. Staudacher, P. Bachélery, and V. Cayol. Formation of the april 2007 caldera collapse at piton de la fournaise volcano: Insights from gps data. *J. Volc. Geoth. Res.*, 2009.

[55] H. Pinkerton and G. Norton. Rheological properties of basaltic lavas at sub-liquidus temperatures laboratory and field measurements on lavas from Mount Etna. *J. Volcanol. Geotherm. Res.*, 1995.

[56] A. Piombo and M. Dragoni. Evaluation of flow rate for a one-dimensional lava flow with power-law rheology. *Geophys. Res. Lett.*, 2009.

[57] A. Piombo and M. Dragoni. Role of viscous dissipation in the dynamic of lava flows with power - law rheology. *Journal of Volc. and Geotherm. Res.*, 2011.

[58] M. Pompilio, R. Trigila, and V. Zanon. Melting experiments on etnean lavas: the calibration of an empirical geothermometer to estimate the eruptive temperature. *Acta Vulcanologica*, 1998.

[59] C. Proietti. *Multitemporal geometrical analysis and numerical simulation of lava flows: the case of the 2001 Etna eruptions.* PhD thesis, Bologna University, Alma Mater Studiorum, 2007.

[60] C. Proietti, M. Coltelli, M. Marsella, and E. Fujita. A quantitative approach for evaluating lava flow simulation reliability the lavasim code applied to the 2001 etna's eruption. *Geochem. Geophys. Geosyst.*, 2009.

[61] R. Romano and C. Sturiale. The historical eruptions of mt. etna. *Mem. Soc. Geol. It.*, 1982.

[62] R. Romano and C. Vaccaro. The recent eruptive activity on Mt. Etna, Sicily: 1981-1985. *Per. Mineral.*, 1986.

[63] S. K. Rowland and G. P. L. Walker. Pahoehoe and aa in hawaii: volumetric flow rate controls the lava structure. *Bull. Volcanol.*, 1990.

[64] T. J. O. Sanderson, G. Berrino, G. Corrado, and M. Grimaldi. Ground deformation and gravity changes accompanying the march 1981 eruption of mount etna. *J. Volc. Geoth. Res.*, 1983.

[65] S. Santini, A. Tallarico, and M. Dragoni. Magma ascent and effusion from a tensile fracture propagation to the earthâ^{TM}s surface. *Geophysical Journal International*, 2011.

[66] S. Scifoni, M. Coltelli, M. Marsella, C. Proietti, Q. Napoleoni, A. Vicari, and C. Del Negro. Mitigation of lava flow invasion hazard through optimized barrier configuration aided by numerical simulation: The case of the 2001 etna eruption. *J. Volcan. and Geothermal Res.*, 2010.

[67] S.C. Scott. Variation in lava composition during the march 1981 eruption of mount etna and the implications of a compositional comparison with earlier historic eruptions. *Bull. Volcanol.*, 1983.

[68] L. Smethurst, M. R. James, H. Pinkerton, and J.A. Tawn. A statistical analysis of eruptive activity on mount etna, sicily. *Geo. J. Int.*, 2009.

[69] I. Sonder, B. Zimanowski, and R. BÃ$\frac{1}{4}$ttner. Non-newtonian viscosity of basaltic magma. *Geophys. Res. Lett.*, 2006.

[70] W. Spataro, D. D'Ambrosio, R. Rongo, and G.A. Tronfio. An evolutionary approach for modelling lava flows through cellular automata. *Lect. Notes Comput. Sci.*, 2004.

[71] F.J. Spera, A. Borgia, J. Strimple, and M. Feigenson. Rheology of melts and magmatic suspensions. 1. design and calibration of a concentric cylinder viscometer for application to rhyolitic magma. *J. Geophys. Res.*, 1988.

[72] T. Staudacher, V. Ferrazzini, A. Peltier, P. Kowalski, P. Boissier, P. Catherine, F. Lauret, and F. Massin. The april 2007 eruption and the dolomieu crater collapse, two major events at piton de la fournaise (la reunion island, indian ocean). *J. Volc. Geoth. Res.*, 2009.

[73] D. A. Swanson, D. B. Jackson, R. Y. Koyanagi, and T. L. Wright. The february 1969 east rift eruption of kilauea volcano, hawaii. *U.S. Geol. Surv. Prof. Paper*, 1976.

[74] A. Tallarico and M. Dragoni. A three-dimensional bingham model for channelled lava flows. *J. Geophys. Res.*, 2000.

[75] J. C. Tanguy, M. Condomines, M. Le Goff, V. Chillemi, S. La Delfa, and G. Patané. Mount etna eruptions of the last 2,750 years: revised chronology and location through archeomagnetic and 226ra-230th dating. *Bull. Volcanol.*, 2007.

[76] H. Tazieff. An exceptional eruption: Mt. nyiragongo, january 10th, 1977. *Bull. Volcanol.*, 1977.

[77] A. Vicari, A. Herault, C. Del Negro, M. Coltelli, M. Marsella, and C. Proietti. Modelling of the 2001 lava flow at etna volcano by a cellular automata approach. *Environ. Model. Softw.*, 2007.

[78] L. Villari. 1981 Etna report, CNR-IIV open file report. Technical report, CNR, 1983.

[79] G. Wadge. The storage and release of magma on mount etna. *J. Volc. Geoth. Res.*, 1977.

[80] G.P.L. Walker. Compound and simple lava flows and flood basalts. *Imperial College. London*, 1971.

*